An investigation into the effects of macromolecular crowding on the kinetics of upper glycolytic enzymes in *Saccharomyces cerevisiae*

by

Julian Wissing

Thesis presented in partial fulfilment of the requirements for the degree of Master of Science (Biochemistry) in the Faculty of Science at Stellenbosch University

Supervisor: Prof. J.M. Rohwer

March 2020

Declaration

By submitting this thesis electronically, I declare that the entirety of the work contained therein is my own, original work, that I am the sole author thereof (save to the extent explicitly otherwise stated), that reproduction and publication thereof by Stellenbosch University will not infringe any third party rights and that I have not previously in its entirety or in part submitted it for obtaining any qualification.

Date: March 2020

Acknowledgements

I would like to express my sincere gratitude to the following people and organisations:

Professor Johann M Rohwer, without whose guidance and support this project would not have been completed.

Arrie Arends for running the lab so astutely and for being a much needed adviser in a pinch.

My beautiful girlfriend, Mianca Teifel, for all of her support and whose continuous love and belief in me which gave me the necessary strength to complete this project.

My mother and father for their undying support, love and encouragement, allowing me to pursue my goals.

My closest friend, Christoff Odendaal, for always being there when I needed motivation and making the late nights in the laboratory bearable.

My friends, who have become my second family and were always able to place a smile on my face when I needed it.

The University of Stellenbosch for use of its facilities and making this project possible.

The National Research Foundation (NRF) for their financial assistance towards this research in the form of a Master's bursary.

Contents

List of Figures

List of Tables

Abbreviations

PGI Phosphoglucose Isomerase

PFK Phosphofructose Kinase

AK Adenylate Kinase

G6P Glucose-6-Phosphate

F6P Fructose-6-Phosphate

FBP Fructose-1,6-Bisphosphate

ATP Adenosine Triphopshate

ADP Adenosine Diphosphate

AMP Adenosine Monophosphate

Summary

In order for mathematical models of metabolism to accurately emulate experimental data the conditions in which parameter values are obtained must be close to the actual *in vivo* environment. However, this is traditionally not the case, with enzyme kinetic studies usually taking place in conditions which are ideal for the enzyme being studied and can be far removed from the actual native conditions the enzyme would be found in. An aspect of the intracellular environment which has not been extensiely covered is the large quantity of different macromolecules which occupy it, known as macromolecular crowding. The space occupied by these macromolecules has thermodynamic and kinetic consequences which are not taken into consideration. In this study we mimicked a crowded environment by using the inert polymers PEG 8000 and Ficoll 70 and studied how they affected enzyme kinetic parameter estimates at different concentrations. NMR spectroscopy was used to obtain time-course data for the upper glycolytic enzymes, phosphoglucose isomerase (PGI) and phosphofructokinase (PFK), in cell lysate. Parameter estimates were obtained by fitting NMR time-course data to a kinetic model based on rate equations for the two enzymes. The identifiability of each parameter was also determined and could be used to analyse the accuracy of parameter estimation. The aim of this study was to determine the effects of macromolecular crowding on enzyme kinetics and to explore if these effects should be considered when trying to simulate *in vivo*-like conditions when studying enzyme kinetics. In our results macromolecular crowding was shown to affect the parameter estimates for both enzymes, in particular decreasing their maximal activity, increasing the binding affinity of PFK for fructose-6-phosphate (F6P), and decreasing its affinity for adenosine tri-phosphate (ATP).

Chapter 1

Introduction

Systems biology aims to understand the emergent properties of a system that are not apparent from observing its constituent parts in isolation [1]. This is applied to studying metabolic pathways where mathematical models are built using enzyme kinetic data. Gathering enzyme kinetic data in solutions that do not emulate the *in vivo* conditions in which these reactions would normally take place may lead to discrepancies between mathematical models and experimental data [2]. Additionally, the lack of a standard assay medium in which to study enzyme kinetics makes the use of kinetic data obtained from other laboratories difficult [2]. Efforts have been made to create standardized buffers to study enzyme kinetics [3; 4]; however, though they do attempt to emulate the large quantity of macromolecules that are in the intracellular environment, these studies only looked at the effects on the V_{max} of the reactions. Traditionally, enzyme kinetic studies take place in solutions where crowding is negligible, containing as little as 1-10 g/L macromolecules, ignoring the thermodynamic and kinetic consequences of the "crowded" intracellular environment in which these reactions actually take place. The intracellular environment is not bulk water occupied with a small amount of diluted solutes; in fact, it is an intensely crowded environment filled with many macromolecules (proteins, polysaccharides, DNA, etc.) where the concentration of macromolecules is between 50 and 400 g/L [5]. The intracellular milieu is a complex environment filled with an abundance of macromolecules. A solution with a large fraction occupied by macromolecules is described as being crowded rather than concentrated as no single molecule may be at a high concentration [6]. These macromolecules take up space in this crowded environment and indeed add to the crowded nature as the already occupied volume the macromolecule resides in is not able to be occupied by another molecule. This can have drastic thermodynamic and kinetic consequences and serves as the basis of excluded volume theory [5–7]. That the "crowded" environment can change how proteins behave has been known for some time [8] though it remains somewhat overlooked when studying enzyme kinetics.

The preferred method for determining kinetic parameters has traditionally been to use initial rate analysis [9], for example determining maximal rate and half-saturation constants using Lineweaver-Burke plots [10]. Progress curves acquire data of substrate and product concentrations while they are changing and yields

more information per run therefore reducing the work-load [11]. Ultimately the type of analysis will determine which method is used [10]. A methodology using ^{31}NMR progress curves to study enzyme kinetics of glycolytic enzymes in *Escherichia coli* has been established [12] and was adapted for this study. A problem which arises in experimental design when fitting to experimental data is that of parameter identifiability [13]. The rise in complexity of the models being studied means that determining the identifiability of parameters has become more important as an identifiability analysis can infer how well a parameter is determined based on the experimental data [13]. Parameters are said to be identifiable, but a parameter may also be structurally non-identifiable, which is a property of the model itself and usually arises due to redundant parameters [13], or practically non-identifiable, which arises due to insufficient quality data [13].
This study investigated the effects of macromolecular crowding on the enzyme kinetics of two glycolytic enzymes, phosphoglucose isomerase (PGI) and phosphofructokinase (PFK). This forms part of a larger investigation of all glycolytic enzymes under crowded conditions in order to determine if macromolecular crowding should be incorporated into a standard kinetic assay solution. The identifiabilty of the fitted parameters was also studied.

Progress curve data was generated using ^{31}P NMR spectroscopy to study the reactions of PGI and PFK. Data collected using this technique are information-rich as they are able to quantify various substrates, products, and allosteric modifiers of these reactions simultaneously. PGI has reversible uni-uni enzyme kinetics while PFK has irreversible bi-bi kinetics. PGI catalyzes the reversible interconversion of glucose-6-phosphate (G6P) to fructose-6-phosphate (F6P)

$$\text{G6P} \leftrightarrows \text{F6P} \tag{1.1}$$

while PFK catalyzes the phosphorylation of F6P to fructose-1,6-bisphosphate (FBP).

$$\text{F6P} + \text{ATP} \rightarrow \text{FBP} + \text{ADP} \tag{1.2}$$

PGI parameter values were determined in isolation by excluding co-factors of adjacent enzymes, while PFK could not be studied in isolation as the reverse reaction of PGI was favoured and converted F6P back into G6P before PFK was able to proceed. The PFK catalyzed reaction was therefore studied as part of a combined PGI-PFK module. After time-course data was collected, parameter values were estimated by fitting the NMR time-course data to simulated model data generated from the relevant rate equations. The commonly used crowding agents, polyethylene-glycol (PEG) 8000 and Ficoll 70, were used to increase the amount of macromolecules in solution in which the PGI and PFK reactions took place. Changes in reaction parameters due to increasing macromolecular crowding were determined by studying the reactions at various concentrations of crowding agents. The effects of different types of crowding agents on kinetic parameters were also determined. Profile-likelihood plots were generated for each parameter to test identifiablity. For parameters which were identifiable, confidence intervals could be generated indicating the accuracy of the fitted parameter value. The objectives of this study can therefore be summarized as follows:

- Establish reference parameter estimates for PGI and PFK in *Saccharomyces cerevisiae*.
- Investigate changes in parameter estimates under crowded conditions.
- Conduct a comparative identifiability analysis of all parameter estimates from progress curve data.

This thesis begins with an introduction to macromolecular crowding theory and a brief discussion on parameter fitting and identifiability analysis in Chapter 2. Chapter 3 describes the experimental procedures used in this study including experimental protocols and data analysis. Chapter 4 summarizes the results from the analysis of experimental data. The discussion of the results in the context of current literature is presented in Chapter 5.

Chapter 2

Literature review

This chapter provides an overview of the literature on the topic of macromolecular crowding, with particular emphasis on its effect on enzyme kinetics as pertaining to the present study. We have also included a short review on parameter estimation and identifiability analysis as this formed the basis for determining kinetic parameters in this study under various macromolecular crowding conditions.

2.1 Macromolecular crowding

Systems biology aims to create accurate, predictive models of reactions which take place inside the cell [14]. For these models to be truly accurate they must reflect the actual conditions in which they would be found. Additionally the lack of a standardized experimental procedures makes it difficult to incorporate experimental data from other laboratories into models.

The term macromolecular crowding has been in use since 1981 [6] to describe the influence on biological processes in a highly-occupied volume consisting of functionally unrelated macromolecules [15]. Current understanding of macromolecular crowding is that it consists of various different factors including: excluded volume, non-specific interactions, and solvent properties [16].

The extent to which the inside of a cell is crowded is not uniform throughout the cell, creating microenvironments where the proteins are affected differently by macromolecular crowding. This adds to the complexity of the crowded environment inside the cell. This complex environment consists of many different biomolecules of varying shapes and sizes has traditionally made it difficult to measure the effects of macromolecular crowding on protein stability inside the cell [17]. The large number of variables that need to be taken into account when performing experiments inside the cells makes it difficult to determine their outcomes [18]. Therefore, in order to simulate the crowded environment in the laboratory, inert polymers such as Ficoll, dextran, or polyethylene glycol (PEG) have been used in solution. Different types of crowding agents have been shown to affect enzyme kinetics differently [19] but that the size of crowding agents does not [20]. Rather it is the volume occupied which has the greater effect on enzyme kinetics [20]. In this study we used two crowding

agents of different sizes and shapes (Ficoll 70 and PEG 8000).

2.1.1 Excluded Volume

The underlying principle of the exclude volume effect is that two molecules in solution cannot occupy the same space and, due to steric repulsion, excludes other molecules from the area around themselves [6]. Traditionally this effect is visualized and modeled using hard spheres [21]. Using this hard sphere model it can be seen that, due to steric repulsion, the closest two molecules can get to each other is the sum of their radii - the excluded volume [22]. Excluded volume is inaccessible to each molecule and by increasing the number of macromolecules present in solution the amount of volume excluded increases [22].

There are important energetic consequences which need to be taken into account when considering the effects of volume exclusion [23; 24]. Macromolecules in crowded solution will be less randomly distributed due to the increase in excluded volume, resulting in a loss of entropy compared to an ideal solution [22]. A consequence of this entropy decrease is the increase of free energy of solutes [22]. Excluded volume has been shown to have a greater effect on larger molecules [25]. If the molecule which is introduced to the solution is of similar size to the crowding agents then the available volume is much smaller than would be expected if the molecule was small as they would easily be able to diffuse between the larger crowding molecules [26].

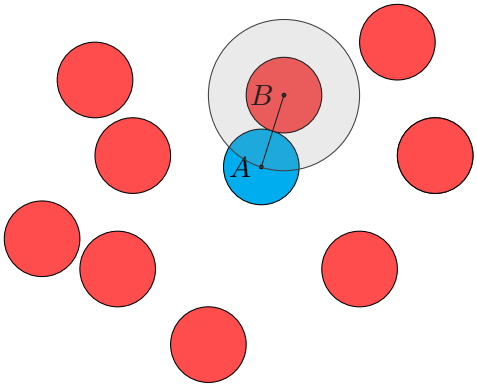

Figure 2.1: A 2-dimensional representation of excluded volume in the crowded solution. The crowding agents (red) and protein of interest (blue) are shown as hard spheres and are the same size. The area excluded by crowding molecule B on A is represented by a grey circle with a radius equal to the sum of the radii for molecules A and B.

2.1.2 Protein folding and association

Proteins favour a native folded state inside a crowded environment due to the excluded volume effect [6]. Increasing the amount of crowding agents in solution reduces

the configurational entropy of the unfolded state of the protein and shifts the equilibrium to favour the native folded state [6]. The excluded volume effect also favours protein-protein association including dimerization. When two monomers come together to form a dimer, excluded volume is reduced, which is energetically favoured [6]. When macromolecules associate the total area accessible to the crowding agents is increased; which leads to the total free energy of the system decreasing due to an increase in entropy [23; 27]. This promotes processes which reduce the volume occupied by favouring the compact state of proteins and association between them. The heterogeneity of macromolecules found inside the cell with large variance of size and shape may enhance protein stabilization when compared to that of a crowded environment which is homogeneous [28].

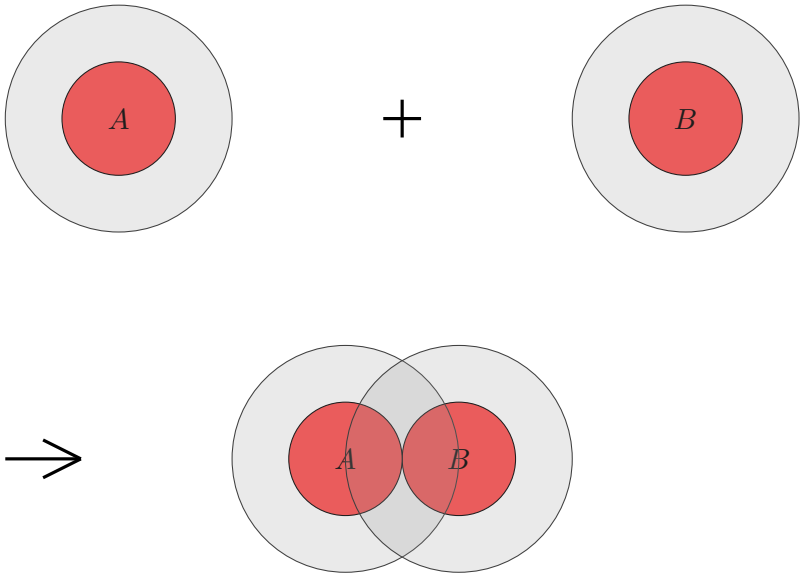

Figure 2.2: The association of two macromolecules (A and B, both in red) will result in less excluded volume. The associated molecule AB will be favoured in a highly crowded environment as the total excluded volume will be less than if the two molecules are disassociated. Excluded volume of each molecules is given by the grey circles.

2.1.3 Non-specific chemical interactions

Most of the research on macromolecular crowding focuses on the effects of steric repulsion from the excluded volume effect due to its generality, ubiquity and its ease to study [29; 30]. However, phenomena such as the destabilization of proteins in highly crowded environments cannot solely be caused by volume exclusion and have been attributed to weak interactions between different proteins [31]. Recently there have been attempts to incorporate these non-specific chemical interactions into the theory of macromolecular crowding [16; 31–36]. The energetic contributions of these interactions in the system are dependent on the type of biomolecule, crowder, and solvent and their contribution to the enthalpy in the system can either enhance or negate the stabilizing effect of steric repulsion depending on the type of interaction observed

[32]. These interactions are weak, but become significant at higher concentrations, therefore, the amount of solvent accessible surface area on a protein determines how great the interaction is, with proteins with a larger surface area accessible to solvent having stronger interactions [30].

Repelling interactions such as electrostatic repulsion enhance the stabilization due to volume exclusion as reactions which involve folding or association generally lead to products with a decreased surface area available to solvent and a reduction in the repulsion between crowding agents and reagents [32]. Attractive electrostatic and hydrophobic interactions can counter the stabilization from steric repulsion and can destabilize proteins [37].

2.1.4 Diffusion

In addition to the excluded volume effect that is present in a highly crowded environment, other effects arise due to a crowded solution. One of these is the result of increased viscosity, which affects diffusion rates of molecules in the solution [25]. In crowded solutions the large amount of macromolecules negatively affects how freely the protein of interest is able to diffuse by acting as obstacles in its path, reducing its mobility [38; 39]. As a consequence diffusion in the cytoplasm is between 3 and 5 times slower than in water [39; 40]. Though all biochemical reactions rely on diffusion as a means of transport to facilitate encounters between enzyme and substrate to some extent [40], changes in the diffusion of molecules will have the largest effect on the kinetics of biochemical reactions which have these encounters as their rate-limiting step and it seems that macromolecular crowding mostly affects the diffusion of large macromolecules [16; 41], though slower diffusion of smaller molecules has also been observed [38]. The size and the amount of crowding agents in solution seem to have some effect on the diffusion characteristics of the tracer molecule [39; 42; 43].

2.1.5 Physiological relevance

The intracellular environment is highly crowded and it is in this crowded environment where enzymes evolved. It has been suggested that the non-covalent molecular forces from macromolecular crowding may have played an important role in the evolution of molecules and the emergence of life through the promotion of self organization and molecular recognition [44]. Additionally, macromolecular crowding may have important, physiological purposes and may be an important factor when considering protein function inside the cell [25]. Macromolecular crowding has also been suggested to have an important role in the formation of large intracellular structures such as the cytoskeleton and chromosomes whose formation may be dependent on forces associated with macromolecular crowding [45].

It has been suggested that macromolecular crowding may play an important role in maintaining homeostasis and offsetting the influence of changes in intracellular volume caused by stress from the environment [25]. One study postulated that macromolecular crowding may serve a role in activating membrane transporters in dog red cells [46]. They claimed this to be due to changes in cellular volume leading

to changes in protein concentrations which can cause protein function to be altered. More recently it has been proposed that macromolecular crowding acts as a mechanism in which yeast cells regulate their biophysical properties in response to glucose starvation in order to maintain homeostasis [47]. They observed that mobility of macromolecules was restricted when yeast cells were exposed to glucose starvation and proposed that this was most probably due a decrease in the intracellular volume and therefore an increase in macromolecular crowding. They reported a 15% reduction in cell volume under glucose starved conditions with no difference in the actual cell mass leading to an increase in macromolecular crowding and therefore changes in the mechanical properties of the cells via regulation of intracellular diffusion and interactions inside the cell [47].

The crowding conditions inside the cell have also been shown to change with osmotic stress [48; 49]. These changes in the crowding environment in the cell may be a means for mammalian cells to protect themselves from osmotic stress by favouring the assembly of mRNA stress granules, increasing their chances for survival [50]. Macromolecular crowding may also be a means for the cell to control intracellular reactions in different regions inside the cell [34]. The stability and folding of the yeast phosphoglycerate kinase (PGK) has been demonstrated to be cell-cycle dependant [51] and has also been shown to change in different localized regions inside the cell. These regions have different levels of crowding and the difference in the localized crowding conditions change the stability and folding of a protein [52]. Interestingly it has been suggested that yeast cells are able to store and inactivate metabolically important enzymes such as glutamine synthase in filaments during cellular starvation in a process which is highly dependant on macromolecular crowding [53].

Macromolecular crowding as a component in maintaining proper cellular function has been established, leading some to hypothesise that microorganisms maintain "crowding homeostasis" via osmolyte transport control or nutrient-dependent regulation of cell size. [24].

2.1.6 Effect on enzyme kinetics

Numerous studies have been attempted to establish how enzyme kinetics change in highly crowded environments. These studies often focused on enzymatic reactions which follow traditional Michaelis-Menten reaction kinetics; how the crowded environment effects these reactions is summarized in Table 2.1. Generally the maximum velocity, V_{max}, of the reactions tends to decrease when the environment these reactions take place in becomes more crowded [54–56] and the affinity of an enzyme to bind to substrate, the Michaelis constant K_m, may either increase [57], decrease [54–56; 58], or remain constant [55].

Whether a certain reaction is diffusion controlled or activation controlled seems to determine how the reaction will be affected by macromolecular crowding [18]. In reactions which are diffusion controlled the limiting factor in the reaction is the enzyme-substrate encounter. The increased volume occupied by crowding agents leads to a change in the diffusion properties and decreases the frequency of encoun-

ters between the enzyme and substrate [18; 57] and should theoretically lead to an increase in the K_m. Another factor which may be responsible for an increase in K_m is modification of the chemical activity of substrate due to the non-ideal conditions as the K_m is sensitive to changes in sample composition [55].

In reactions which are activation controlled the change in diffusion properties will not affect the reaction rate as the the limiting factor is the conversion of substrate to product. Instead, at higher concentrations of crowding the effective concentrations of the substrate and the protein increase which is expected to cause the K_m of the reaction to decrease as the affinity for the substrate to the enzyme increases. Conformational changes of the enzyme has also been suggested to cause a decrease in K_m [54; 57]. In isochorismate synthase (EntC) the K_m decreased and the enzyme was observed to undergo conformational changes due to the excluded volume effect in increasing concentrations of the crowding agent Ficoll 70 [54].

The crowded environment affects the maximum velocity (V_{max}) in different ways. As has been discussed previously, volume exclusion changes the equilibrium of self-association of the enzymes and may induce conformational changes which may lead to changes in the active site and therefore change the V_{max} [18; 20; 59]. Whether these conformational changes lead to an overall increase or decrease in the V_{max} of a protein is difficult to predict as the conformational change can either favour or hinder the interactions between enzyme and substrate [20].

An increase in V_{max} can be the result of an increase in the effective concentration of the enzyme [18]. This makes sense when one considers that the V_{max} is defined by the product of the catalytic rate constant (k_{cat}) and the enzyme concentration.

The substrates and products of enzymatic reactions make an insignificant contribution to excluded volume in the system as they are usually very small [55]. These small molecules are generally unaffected by the increase in viscosity of these environments [54].

In general V_{max} and K_m both decrease when an enzyme reaction takes place in a crowded environment. Though these relationships generally hold true, other factors such as the type and size of the crowding agent used in the study, can lead to differing results, adding further complexity to studying enzymes in crowded conditions [20; 55; 60]. The size of the crowding agent used in the study appears to have an effect on the stabilization of the enzymes, with smaller crowding agents being shown to have a greater stabilization effect on lysozyme and α-lactalbumin [28]; however structure and function of a protein appears to be determined by the amount of volume being excluded [20; 60]. The reaction rates of small enzymes are only influenced by the actual amount of excluded volume, whereas bigger enzymes are affected by the size of the crowding agents as well [20; 55; 56].

Though there has been much work to grow our understanding of how macromolecular crowding affects enzyme kinetics, how these kinetics are affected appears to change dramatically from enzyme-to-enzyme.

Table 2.1: Summary of published data for kinetic parameters of various enzymes in "crowded" conditions, including the organism from which the enzyme is sourced and the crowding agent used in the study. ↑ and ↓ indicate an increase or a decreased respectively of the enzyme parameters in "crowded" solution. – indicates that no change in the parameter was observed.

Enzyme	Organism	Crowding Agent	K_m	k_{cat}	Reference
L-lactate dehydrogenase	Rabbit muscle	Dextran	↓	↓	[55]
α-chymotrypsin	Bovine pancreas type II	Dextran	↑	↓	[20]
Peroxidase	Horseradish	Dextran	↓	↓	[20]
L-lactate dehydrogenase	Rabbit muscle	Dextran	↓	↓	[20]
Malate dehydrogenase	Mitochondria	Dextran	↓	↓	[56]
		Lysozyme	↓	↓	[56]
Malate dehydrogenase	*Thermus flavus*	Dextran	↑	↓	[56]
		Lysozyme	–	↓	[56]
Isochorismate synthase	*Escherichia coli*	Ficoll	↓	↓	[54]
Fet3p	*Saccharomyces cerevisiae*	Ficoll	↓↑	↓↑	[57]
ADP-sugar pyrophosphatase	*Escherichia coli*	PEG	↑	↑	[58]

2.2 Brief overview of systems biology

The shift towards a systems biology approach in studying biological phenomena has been deemed necessary as traditional reductionist techniques, which dominated in the previous century, lack the means to study biological characteristics which cannot be attributed to a single molecule [61]. The emphasis in systems biology is therefore placed on viewing the constituents of a system in the context of the system itself rather than in isolation and it therefore makes it possible to observe emergent properties which may lead to a better understanding of the function of the system [14]. Even with a complete knowledge of the genome of an organism and the crystal structures of all its proteins, without an understanding of how they interact with each other very little information regarding function can be determined [62]. In order to achieve this, systems biology uses a combination of mechanistic information derived from traditional molecular biology techniques and analysis techniques from mathematics [63]. The result of the integration of biological data is the formation of powerful mathematical models which can help to elucidate biological function.

There are two different approaches to tackle the challenge of developing and curating models to gain intimate knowledge of bioglogical phenomena: the top-down approach where large "omics" datasets are used to infer and understand their underlying relationships [64]; and the bottom-up approach where the constituent parts of a system are observed experimentally and are then incorporated into a model of a larger system [62].

Top-down systems biology approaches incorporate large genome-wide experimental data in order to discover molecular mechanisms. Since they are genome-wide, top-down models are potentially complete [62]. Top-down techniques involve the collection and analysis of a data set of an organism with set perturbations to determine correlations between concentrations of molecules, which are used to formulate

an hypothesis regarding the regulation of these molecules. The hypothesis is then tested by another set of experiments involving a different set of perturbations [62].

The bottom-up approach aims to make accurate models via the formulation of mathematical relationships between the constituent parts of the model. The bottom-up approach was used in this study and incorporates parameters found experimentally or in literature into rate equations. The rate equations can then be used to formulate a kinetic model of the system under investigation [62]. Though more labour intensive, because the models are constructed using the direct data of their constituent components, the model should be more accurate and have increased predictive power [12] than models constructed using the top-down approach.

2.2.1 Construction of models

A kinetic model is described by its constituent reactions. Each of these reactions is in turn described using a rate equation. The construction of a kinetic model requires five types of data and has been reviewed in [65]. In summary the data that is required consists of:

- stoichiometric data - data which describes the number of compounds involved in the model and the nature of their interactions;
- enzyme kinetic data - consists of the the rate laws for each enzyme and the parameters which describe them. These include the Michaelis-Menten constant, inhibition and activation constants among others [65]. If parameters cannot be determined experimentally there exist databases such as BRENDA [66] and SABIO-RK [67] which can be used to find the relevant kinetic data. Parameters obtained under conditions similar to those found *in vivo* are preferred, however this has not been historically the case [3]. See also Section 2.2.3;
- thermodynamic data - should be incorporated when possible as it gives information regarding the reversibility of each reaction. This will affect the direction of the reactions in the model;
- maximal enzyme activity - the data concerning the maximal enzyme velocity should be acquired under the specific biological conditions for which the model is being described. As this is directly dependent on concentration of enzyme it is not readily transferable between laboratories and conditions;
- other model parameters required to construct the model. These usually take the form of fixed parameters, sink metabolites, and the sum of moiety conserved species such as the nicotinamide adenine dinucleotide redox couples or ATP and ADP.

In order to use a mathematical framework to determine the interactions between components of a system, enzymatic rate equations for each enzyme in the biological network are incorporated into the model as a series of ordinary differential equations (ODEs) [68; 69]. Each ODE in the system is calculated as a rate of change of a metabolite in the network and is determined by taking the sum of rates of reactions

that produce that metabolite minus the sum of rate of reactions that consume the metabolite. Once the model of the system has been developed it must then be validated by using independent data to compare with model output data. This final step is used to test how well the model is able to emulate experimental data, thus ensuring that the model is truly predictive. Since the model is based on inherent enzyme characteristics it can theoretically make predictions in a variety conditions and we may observe emergent properties which would otherwise be difficult to predict [68].

2.2.2 Determining enzyme-kinetic parameters

The parameters for each enzyme in the kinetic network need to be determined in order for the kinetic model to be biologically relevant. The parameters are often determined by using regression analysis to minimize the difference between experimental and model data [68]. This is usually done using either the maximum likelihood (ML) method; or the least squares (LS) method. In the ML method a parameter value is determined when the value maximizes the probability that the model output data is the the same as the experimental data [68]. This probability is determined as a function of the difference between model predicted data and actual experimental data. The LS method iteratively minimizes the objective function, attempting to find a parameter value which reduces the sum of squares of the difference between model and experimental data. Assuming the experimental noise follows normal distribution, the ML and LS methods are equivalent [68].

Traditionally kinetic data are determined using the initial rates of reactions, determined by techniques such as spectrophotometric assays. The amount of light absorbed by a reagent of the reaction is detected by the spectrophotometer and corresponds to the concentration of that reagent. The concentrations of substrates, products and modifieres determine the rate and the experiment is then repeated at various different concentrations of the reagent. Kinetic parameters can then be determined by fitting a kinetic rate equation to a data set containing the initial rate vs concentration of reagent. This is done for both substrates and products.

Whereas classical assays make use of the initial reaction rates to fit kinetic equations, using nuclear magnetic resonance (NMR) spectroscopy, it is possible to make use of progress curve data consisting of all the metabolites present in the reaction, and because of this each NMR spectrum has a great density of information pertaining to the kinetic characteristics of an enzyme [12]. Fitting these time course data to simulated model data will return the parameter values used to describe that reaction. This method of obtaining parameters from NMR time-course data has been used in previous studies pertaining to the characterization of glycolytic enzymes in *Escherichia coli* [12; 70].

To find the minimum of the objective function various different optimization methods have been developed and fall into one of two classes: global or local.
Local optimization techniques rely on an initial guess for the minimum that is close to the global minimum to avoid converging to a local minimum [71]. Global opti-

mization methods search over the entire parameter space searching for smaller values of the objection function, but unlike local optimization techniques do not converge [71]. As reasonable estimations of the parameters can be derived from literature, local optimization techniques were favoured in the analysis in this study.

2.2.3 *In vivo*-like conditions

Van Eunen *et al.* developed a standardized *in vivo*-like assay medium for the study of enzyme kinetics [3]. In the assay medium they took into careful consideration factors such as anion concentrations and pH, but did not find it necessary to emulate the crowded intracellular environment. They tested PEG and BSA at an unspecified concentration and found that macromolecular crowding had no effect on the V_{max} of glycolytic enzymes [3]. However, they did not take into consideration possible changes in other kinetic parameters such as the half-saturation constant which macromolecular crowding has been shown to affect (discussed in Section 2.1.6), nor did they test other crowding agents. Other studies have shown that the effect of macromolecular crowding on V_{max} and K_m are more pronounced when a greater fraction of the volume is occupied [20; 55]. In order for a standardized assay solution to emulate *in vivo*-like conditions the consequences of the crowded environment inside the cell must be considered for the kinetic parameters to be more biologically relevant. This question is examined in greater detail in this thesis.

2.2.4 Identifiability of parameters

Many biological models contain a large number of parameters [72; 73] which are often only partially observable and may be reliant on species which may not be reliably measured. Additionally, data collected may be unable to sufficiently estimate parameter values as the model may be too large or the quality of data may be insufficient [13; 74]. These parameters are known as non-indentifiable. Models cannot be well constructed without sufficiently good data and well-determined parameters.

Determining identifiability

Once the model data has been fitted to the experimental data and the objective function has been minimized, an identifiability analysis can be performed to determine which parameters are non-identifiable. The profile likelihood method for determining parameter identifiability is introduced here. It is a powerful method, being able to test for structural and practical non-identifiability whilst requiring less computational power than other methods [13]. Other methods include the DAISY method [75], which is an algorithm designed to perform a global parameter identifiability test on polynomial equations, or the EAR approach which involves applying the inverse function theorem to the algebraic equations relating to higher order operatives of the output with respect to time [76].

In the profile likelihood method, a parameter, θ_i, from the set of parameters describing the model, is kept fixed while the other parameters in the set are re-optimized. By repeating this for increasing and decreasing values of θ_i it is possible

to explore the parameter space. Most importantly for this analysis is that non-identifiability will will be represented by a flat line in the parameter space of the likelihood function [69]. If non-identifiable parameters are found it is recommended that one implement an iterative design strategy and repeat the investigation with more data, or remove the redundancy in the model [77].

Since parameters are only identifiable if their confidence intervals are finite, one needs to accurately determine the confidence interval. This can be determined by first calculating a threshold in the likelihood, Δ_α, this corresponds to the 1-α quantile of the χ^2-distribution with one degree of freedom. Likelihood-based confidence intervals use the threshold value to determine the confidence region, where the χ^2 goodness-of-fit statistic of the re-fitted model crosses the threshold.

Non-identifiable parameters can be classified as being either structurally or practically non-identifiable or both [13]. Structural non-identifiable parameters (an example is shown in Figure 2.3 A) are the result of redundancy in the model and changing the value of these parameter does not change the output of the model as other parameters are able to compensate [73; 78]. This is a characteristic of the model itself and is independent of the data. When developing a model to describe biological data, an analysis using generic data can be done prior to experimentation to develop the model and remove redundant parameters [69]. A structural non-identifiable parameter will be represented on profile likelihood plots as a flat valley with no unique minima.

A parameter which is practically unidentifiable is the result of low quality or insufficient data (an example is shown in Figure 2.3 C) [13; 71]. In this case the parameter has one confidence region which is finite and another which extends infinitely. If the threshold is not crossed, but a unique minimimum could be found (as shown in Figure 2.3 D), the parameter is still said to be practically non-identifiable [69]. This may be remedied by increasing the quality or quantity of data. Importantly a unique minimimum could be determined.

If a parameter is both structurally and practically identifiable the threshold is crossed on either side of the fitted parameter when exploring the parameter space (an example is shown in Figure 2.3 B). This corresponds to two confidence intervals [13].

In the next chapter the experimental protocol and the parameter fitting methodologies used in this study will be discussed.

Figure 2.3: Examples of profile-likelihood plots for a parameter which is structurally non-identifiable (A); practically and structurally identifiable (B); and practically non-identifiable (C and D). The profile likelihoods are given by the solid lines and the red dashed lines indicate the threshold value, Δ_α utilized to assess likelihood-based confidence intervals.

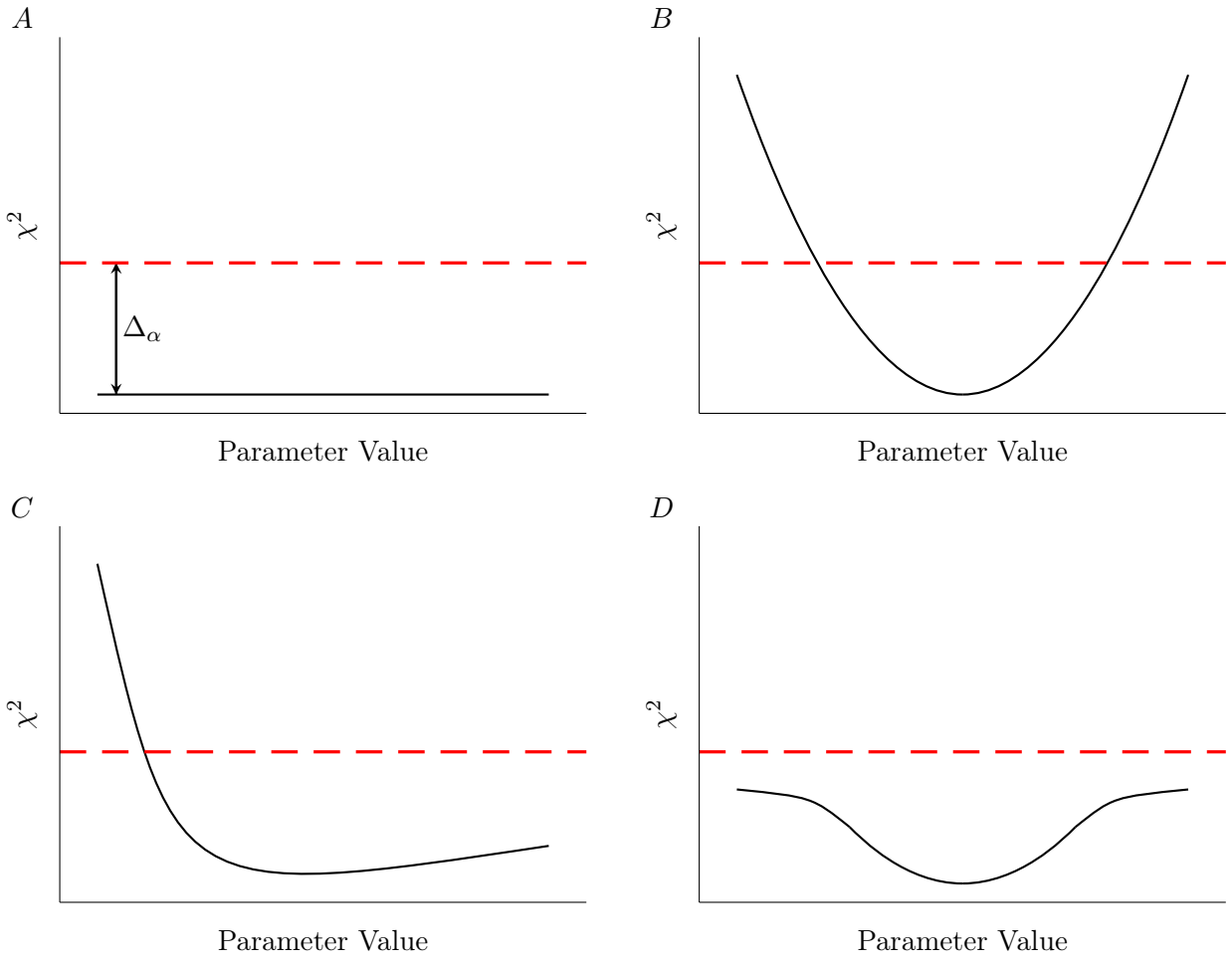

Chapter 3

Methods

3.1 Cell culture and harvest

Freezer stocks of wild type *Saccharomyces cerevisiae* (CEN.PK.113-7D) were grown on agar plates made of 1 g KH_2PO_4, 1 g $(NH_4)_2SO_4$, 0.5 g $MgSO_4 \cdot 7\,H_2O$, 20 g glucose, 10 g yeast extract and 15 g agar per litre at 37°C overnight. To ensure homogeneity of the cells a single colony was then picked from the agar and grown overnight in 50 mL liquid yeast minimal media consisting of 6.7 g/L yeast nitrogen base, 20.44 g/L potassium phthalate and 10 g/L D-glucose at a pH of 5.0 in a 250 mL Erlenmeyer flask. The optical density of the overnight culture was examined and was used to inoculate 3 L of yeast minimal media, ensuring that the starting optical density of the innoculated, final working culture was 0.1 (600 nm).

The working culture was grown until an optical density of 1.0 (600 nm), when the growing culture was in mid-logarithmic growing phase. The liquid media was then placed into falcon tubes and centrifuged using a JA-10 rotor at 12400 $\times$ g for 10 minutes until a pellet was formed. The pellet was then resuspended in 100 mM PIPES buffer (pH 7.0) and 1 mL aliquots were placed in 1.5 mL eppendorf tubes. The aliquots were centrifuged at 4°C at 16100 $\times$ g at 4 °C for 10 minutes. The supernatant was then discarded and the pellets were frozen and kept at -80 °C.

3.2 Cell extraction

To extract lysate from the frozen pellets, they were resuspended in 1 mL of 100 mM Pipes buffer (pH 7.0) and placed it in a 10 mm glass test-tube with 1g glass beads (425-600 µm) from Sigma. Glass bead extraction was done by vortexing for 30 seconds at full speed and then cooling in ice for 30 seconds to avoid overheating. This was repeated for 8 minutes after which the contents of the glass test-tube were then decanted into 1.5 mL eppendorf tubes which were centrifuged for 10 minutes at 16100 $\times$ g at 4 °C. The supernatant was then extracted to be used for analysis. Protein concentration of cell lysate was determined using Bradford assays [79] and comparing to a standard dtermined from bovine serum albumin (BSA).

3.3 NMR spectroscopy

A total of 6-12 assays were completed for the phosphoglucose-isomerase (PGI) and phosphofructokinase (PFK) catalyzed reactions at various starting concentrations of substrate, product and co-factors using buffer solutions consisting of various concentrations of the inert polymers Polyethylene glycol (PEG) 8000 (from Sigma-Aldrich) and Ficoll 70 (from GE Healthcare) to emulate crowding conditions. Crowding agents were dissolved in 100 mM PIPES at the necessary concentrations.

All reaction components were obtained from Sigma-Aldrich and were dissolved in 100 mM PIPES buffer (pH 7.0) to ensure pH homogeneity of the final solution. For the PGI catalyzed reaction G6P and F6P were used as substrates for the forward and reverse reactions respectively at various concentrations ranging from 2.5 mM to 30 mM. For the PFK catalyzed reaction, F6P was used as substrate at starting concentrations between 2.5 mM and 15 mM along with 5 mM ATP. Final samples were prepared in 5 mm NMR tubes and including all substrates, products and co-factors necessary for the reaction to take place, 100 µL triethyl phosphate (TEP) (50 mM) as an internal standard, 10% D_2O and 50 µL $MgCl_2$ (50 mM). The remaining volume was filled with PIPES buffer containing the relevant crowding agent until the final volume of the sample was 1 mL. The cell lysate was added to start the reaction with the final range of protein concentration being between 0.3 $mg \cdot mL^{-1}$ and 1.5 $mg \cdot mL^{-1}$.

All ^{31}P NMR assays were performed on a Varian 400 MHz spectrometer, at 25 °C at a frequency of 161.89 MHz; spectra were collected with a Free Induction Decay (FID) with a pulse angle of 90 °with proton decoupling and no Nuclear Overhauser Enhancement (NOE). The repetition time for a FID was 2.4 min, made up of 12 transients with a relaxation delay of 12 s between transients. If a species is not fully relaxed before the next FID is acquired it may result in a decay of the FID and the integrated metabolite concentration will be incorrect. To avoid this, a fully relaxed spectrum (relaxation delay of 60 s with proton decoupling no Nuclear Overhauser Enhancement) was collected at the end of each run when the reaction had reached equilibrium and was used to calibrate any species that were not fully relaxed [12].

NMR peaks of interest were identified by adding 5 mM of the compound of interest to the NMR tube after the run was completed. The NMR spectra were processed using NMRPy, a NMR spectra analysis package developed for the Python software language [12; 80]. For processing, the FIDs were first zero-filled, followed by apodisation (5 Hz) and Fourier transformed to generate arrayed spectra. Phase-correction was done using the automated phase-correction tool supplied by NMRPy, using a mixture of first and zero order phase correction to minimize the total area under the peaks. The concentration of each metabolite in each FID was calculated by deconvoluting its corresponding peak using Lorentzian lineshapes. The integrated metabolite concentrations were then scaled to the internal standard, TEP, to determine their actual concentration value.

3.4 Kinetic models

The reaction rate of the interconversion of G6P to F6P catalyzed by PGI was described using a reversible Michaelis-Menten equation:

$$v_{PGI} = V_f \frac{\left(\frac{g6p}{K_{m,G6P}}\right)\left(1 - \frac{\Gamma}{Keq}\right)}{1 + \frac{g6p}{K_{m,G6P}} + \frac{f6p}{K_{m,F6P}}} \tag{3.1}$$

where Γ is the mass-action ratio between $f6p$ and $g6p$ at any given point in time. The parameter V_f is the maximum rate of the reaction. $K_{m,G6P}$ is the Michaelis constant for G6P, $K_{m,F6P}$ the Michaelis constant for F6P, and Keq is the equilibrium constant of the reaction.

The enzyme PFK catalyzes the phosphorylation of F6P to F-1,6-BP. The forward reaction of PFK is highly favoured which makes it difficult to collect data of the reverse reaction when the reaction is allowed to equilibrate, as the concentrations would be too low to detect [12]. The rate equation for the PFK catalysed reaction was therefore modeled using a bi-bi, irreversible Hill equation [81] with ATP as a negative allosteric modifier:

$$v_{PFK} = V_f \frac{\left(\frac{f6p}{K_{F6P}}\right)^h \left(\frac{atp}{K_{ATP}}\right)^h}{\frac{1 + \left(\frac{atp}{K_{i,ATP}}\right)^h}{1 + \alpha^{4h}\left(\frac{atp}{K_{i,ATP}}\right)^h} + \frac{1 + \alpha^{2h}\left(\frac{atp}{K_{i,ATP}}\right)^h}{1 + \alpha^{4h}\left(\frac{atp}{K_{i,ATP}}\right)^h}\left(\left(\frac{f6p}{K_{F6P}}\right)^h + \left(\frac{atp}{K_{ATP}}\right)^h\right) + \left(\left(\frac{f6p}{K_{F6P}}\right)^h \left(\frac{atp}{K_{ATP}}\right)^h\right)} \tag{3.2}$$

The half-saturation constants for ATP and F6P are given by the parameters K_{ATP} and K_{F6P}, respectively. V_f is the maximum rate of the reaction. ATP also acts as an allosteric inhibitor of the PFK reaction [82] and the half-saturation constant for this interaction is represented by the parameter, $K_{i,ATP}$. The parameter α gives an indication of the effect of the allosteric modifier. If the allosteric modifier is an activator α>1, if it is an inhibitor α<1 [81]. The Hill coefficient is given by the parameter h.

ATP and ADP form complexes with Mg^{2+} in solution (MgATP and MgADP respectively). The MgATP complex acts as the true substrate in the PFK reaction. Simulations were done with literature values for the following complex formations [12; 83]:

$$Mg^{2+} + ATP \leftrightarrows MgATP \tag{3.3}$$

$$Mg^{2+} + ADP \leftrightarrows MgADP \tag{3.4}$$

From the simulations it was found that virtually all of the ATP in solution was in the form MgATP (not shown). Therefore, all ATP and ADP in the solution was modelled as already being in their respective complexes, MgATP and MgADP.

Adenylate kinase (AK) plays an important role in upper glycolysis. It is found in abundance and is responsible for the interconversion of ATP, ADP and AMP:

$$2\text{ADP} \leftrightarrows \text{ATP} + \text{AMP} \tag{3.5}$$

This interconversion allows for the ADP produced during the phosphorylation of F6P to F,1-6,BP to be converted back into ATP. The adenylate kinase catalyzed reaction was modelled in equilibrium with fixed parameters found in literature [84].

3.5 Data fitting

Collected NMR spectra data were analysed using an the NMRpy package developed by Eicher and co-workers [12; 80]. NMRpy fits Lorentzian functions to peaks in the NMR spectra to calculate the area under peaks in the spectra. The given areas correspond to the concentrations of metabolites at that time-point normalised to the internal standard TEP.

All of the data were analysed using the Python programming language inside a Jupyter workbook environment to allow efficient workflow [80] of the data from processing the NMR data and fitting them to the relevant kinetic models in order to predict the necessary kinetic parameters, and determine the identifiability of the found parameters.

Time course data were generated using the Python simulator for cellular systems (PySCeS) [85]. To minimize the model parameter values we used the LmFit [86] package which is a wrapper of the scipy.optimize package. The model was initialised to initial conditions for every NMR run. The simulated data were then fitted to the acquired time-course NMR data using either the Levenberg-Marquardt least squares or the Nelder-Mead simplex method to minimize the difference between the model and acquired time-course data by changing the parameter values. After optimization, the algorithm returned adjusted parameters to describe the acquired time-course data.

3.6 Identifiability analysis

Once parameters were determined the identifiability of each parameter was analysed using profile likelihood plots [13]. To produce the profile-likelihood plots for each parameter, the parameter being tested is kept was kept fixed at varying points between $\frac{1}{10}$ and 10 times the original fitted parameter value and the remaining parameters re-fitted to find the minimum. For each of these iterations a new "χ^2" was generated and compared to the original value,"χ_0^2". Where $\chi^2 - \chi_0^2$ surpassed the threshold value, it corresponded to the 95% confidence region of the value. The threshold value

was calculated as the 0.95 quantile of the χ^2 distribution with 1 degree of freedom. The theory behind this approach has been discussed in Section 2.2.4.

Chapter 4

Results

As was discussed in Section 2.1, the term macromolecular crowding encompasses a variety of effects which an enzyme is subject to due to the large concentration of macromolecules in the intracellular environment. It is an ubiquitous effect, present in all intracellular environments [5] and serves as a major contributor in changing the energetics of a "crowded" environment, which has consequences for enzyme kinetics [26]. Theoretical explanations of the consequences of the "crowded" environment on the kinetic parameters of an enzyme were explored in Section 2.1.6.

This study attempted to determine the effects of macromolecular crowding on the kinetic parameters of the upper glycolytic enzymes phospho-glucose isomerase (PGI) and phosphofructokinase (PFK) in the model organism, *Saccharomyces cerevisiae*.

The NMR time-course data along with the predicted, fitted model data are shown first, followed by the profile-likelihood plots of the identifiability analysis. The final, fitted parameter values for reference conditions as well as at various concentrations of different crowding agents are then presented as well.

4.1 Parameter estimation

In order to observe whether parameter values for the upper glycolytic enzymes, PGI and PFK, changed in the presence of increasing crowding conditions we use standard assay conditions close to physiological conditions [12] to obtain the baseline values for PGI and PFK parameters in an "uncrowded" solution. The PGI parameters were obtained in isolation and were then used to find the PFK parameters in a combined PGI-PFK system (Figures 4.2 and 4.3).

PGI catalyzes conversion of glucose-6-phosphate (G6P) to fructose-6-phosphate (F6P). It is possible to study the enzyme in isolation using cell-extract as the reaction requires no co-factors to proceed while the next enzyme in glycolysis, phosphofructose-kinase (PFK) cannot proceed unless adenosine triphosphate (ATP) is present in the buffer solution. The preceding reaction, hexokinase, is a highly irreversible reaction

and does not proceed in the reverse direction.

To estimate the relevant parameter values for the PGI reaction ^{31}P NMR progress curve data were gathered and fitted to simulated models. PGI time-course data were gathered for both the forward and reverse reactions at various starting conditions of substrate and product.

The PFK enzyme catalyzes the phosphorylation of F6P to fructose 1,6-bisphosphate (FBP). It cannot be studied in isolation in whole-cell lysate as the PGI reaction that precedes it is able to convert F6P back to G6P faster than PFK is able to phosphorylate it into FBP, without requiring any additional co-factors. In order to overcome this, the parameters for the PGI rate equation were determined before proceeding with the PFK reaction. Then, once PGI parameters were quantified, they could be incorporated into a PGI-PFK coupled module and kept fixed, fitting only for the PFK parameters.

Time-course data obtained where both PFK and PGI were active were more complex than those of the PGI time-course alone as can be seen by the congested sugar-phosphate area in Figure 4.1 a. In addition to the two peaks of the two G6P anomers and the single F6P peak produced by the PGI catalyzed reaction the FBP molecule, which is the product of the PFK catalyzed reaction, has two anomers with two phosphate moieties each thus appearing as four distinct peaks in the ^{31}P NMR spectrum. ADP exhibits two peaks and ATP three, one for each phosphate moiety. AMP peaks were not observed. The time course data for the uncrowded data of the PGI-PFK coupled reaction along with the fitted model curves are shown in Figures 4.2 and 4.3.

Ficoll 70 as a crowding agent

To determine the parameter values in "crowded" conditions the PGI-PFK coupled module was re-analyzed in solution containing 10% and 20% Ficoll. This was done to determine how the kinetic reaction parameters change in solutions that contain a large amount of macromolecules, as would be expected *in vivo*. The progress curves for these reactions along with the fitted model curves are shown in Figures 4.4 to 4.7.

PEG 8000 as a crowding agent

PEG 8000 was used as another crowding agent to see if any changes could be observed when a different crowding agent is used to emulate macromolecular crowding effects. The reactions were repeated in buffer solutions containing 10% and 20% PEG 8000. The progress curves for these reactions along with the fitted model curves are shown in Figures 4.8 to 4.11.

Figure 4.1: An example of the PGI-PFK ^{31}P NMR time-course reaction module. Each of the ^{31}P NMR time-course data sets were collected at a 90°pulse angle with 1 s acquisition per transient and 12 s relaxation between transients. (a) shows the sugar-phosphate area of the spectrum (4.2 to 2.7 ppm) containing: FBP-α: 1, 2, 10; FBP-β: 6, 7, 9; G6P-β: 3; G6P-α: 4, 5; F6P: 8. (b) shows the area between -5 and -11 ppm which contains the ATP and ADP species. ATP-γ and ATP-α: 1 and 4; ADP-α and ADP-β: 2 and 3.

(a)

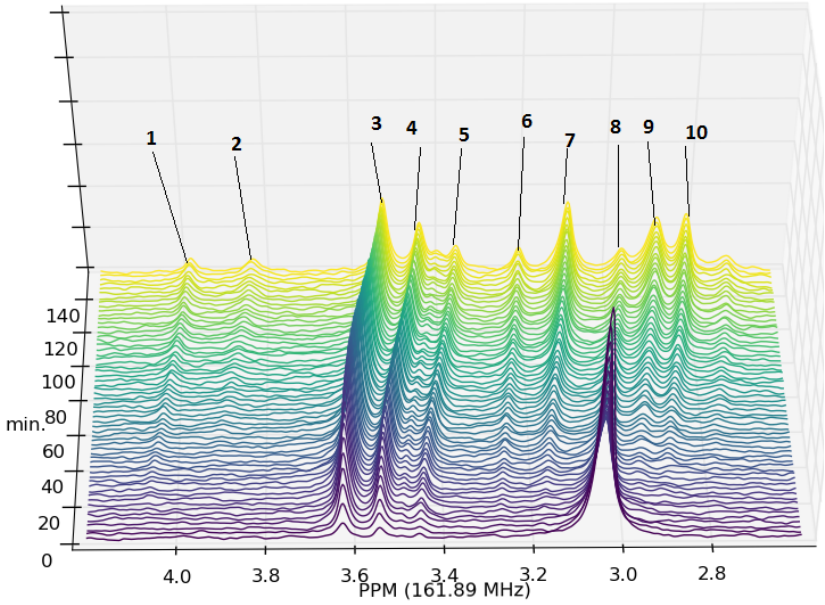

(b)

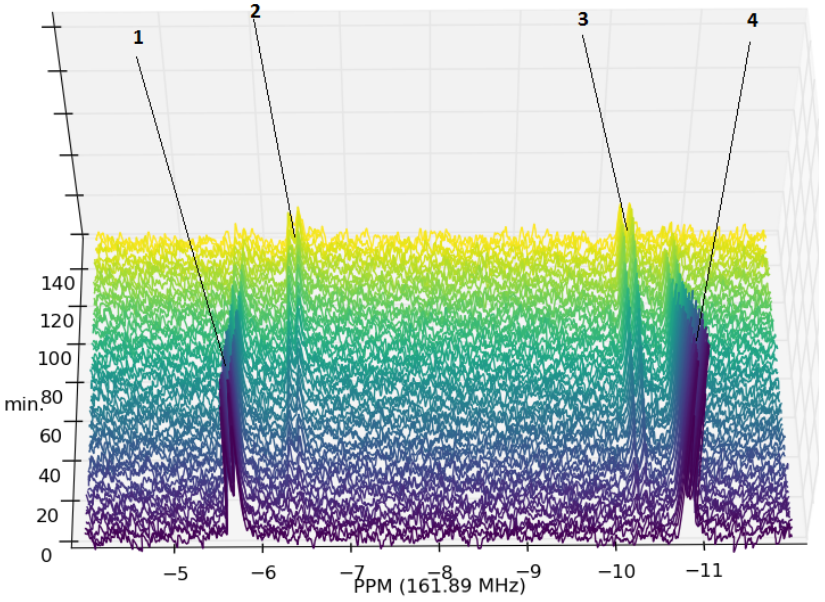

Figure 4.2: Time course data captured for the PGI catalyzed reaction at various initial concentrations in an uncrowded solution. The dotted lines represent experimental NMR data. Solid lines represent a global fit to all the data.

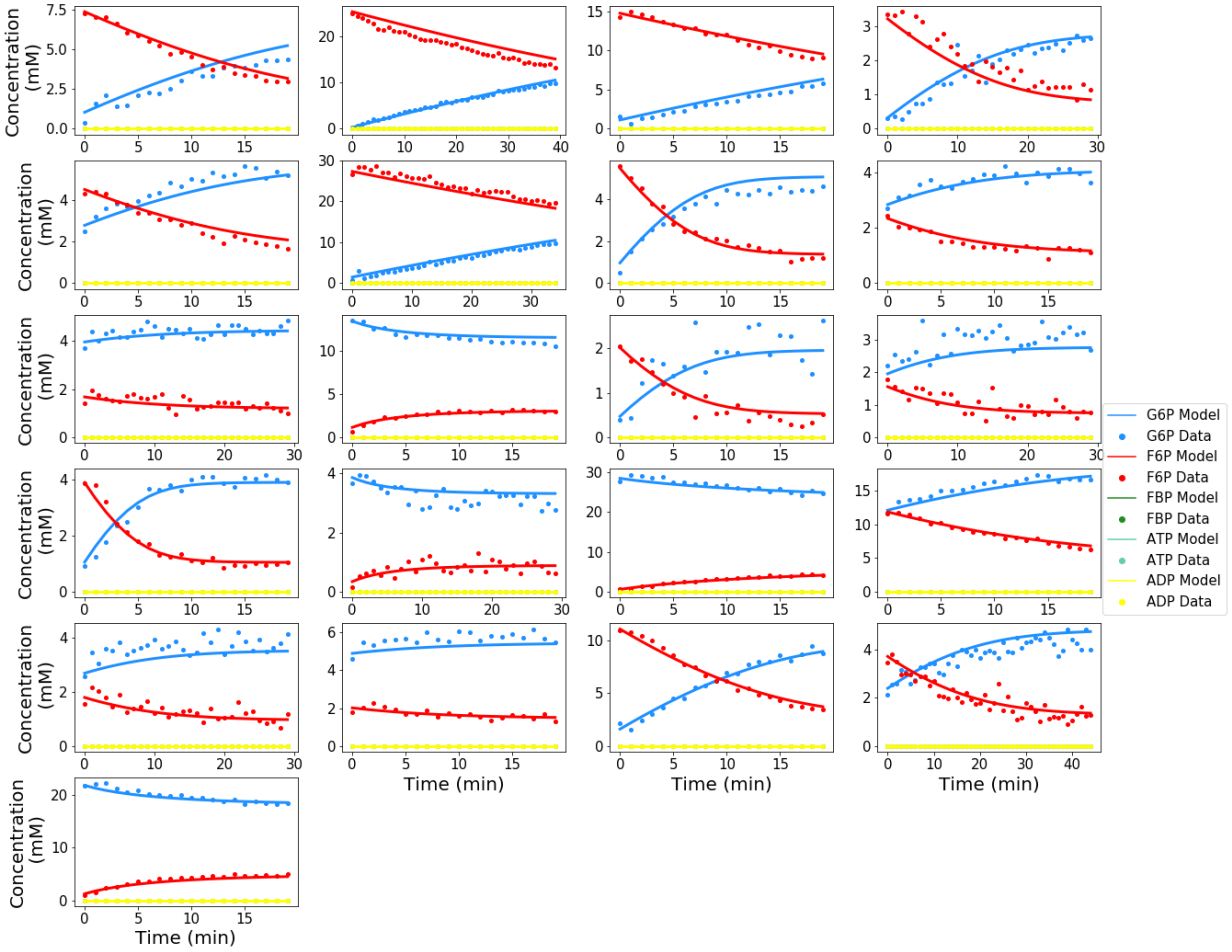

Figure 4.3: Time course data captured for the PGI-PFK catalyzed coupled module at various initial concentrations in an uncrowded solution. The dotted lines represent experimental NMR data. Solid lines represent a global fit to all the data.

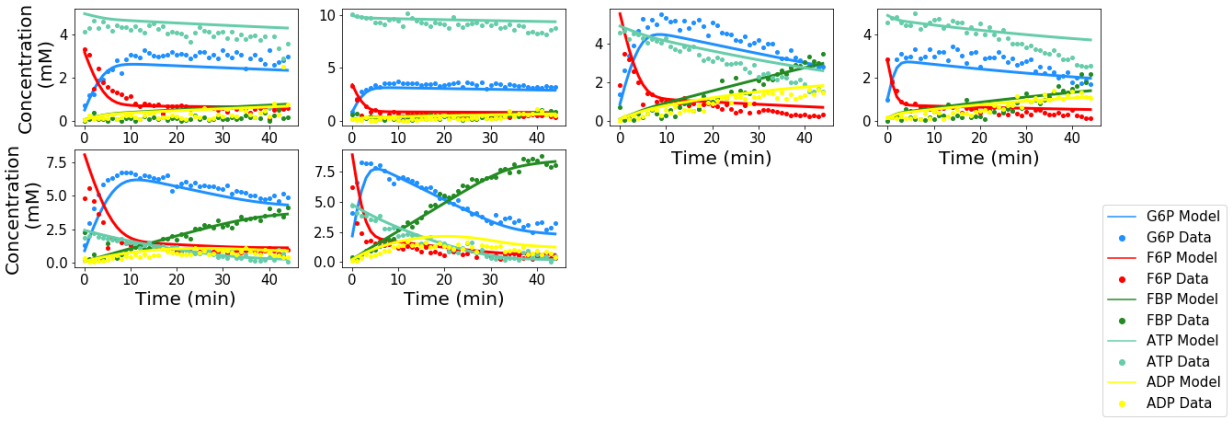

Figure 4.4: Time course data captured for the PGI catalyzed reaction at various initial concentrations using a "crowded" solution with 10% (m/v) Ficoll 70. The dotted lines represent experimental NMR data. Solid lines represent a global fit to all the data.

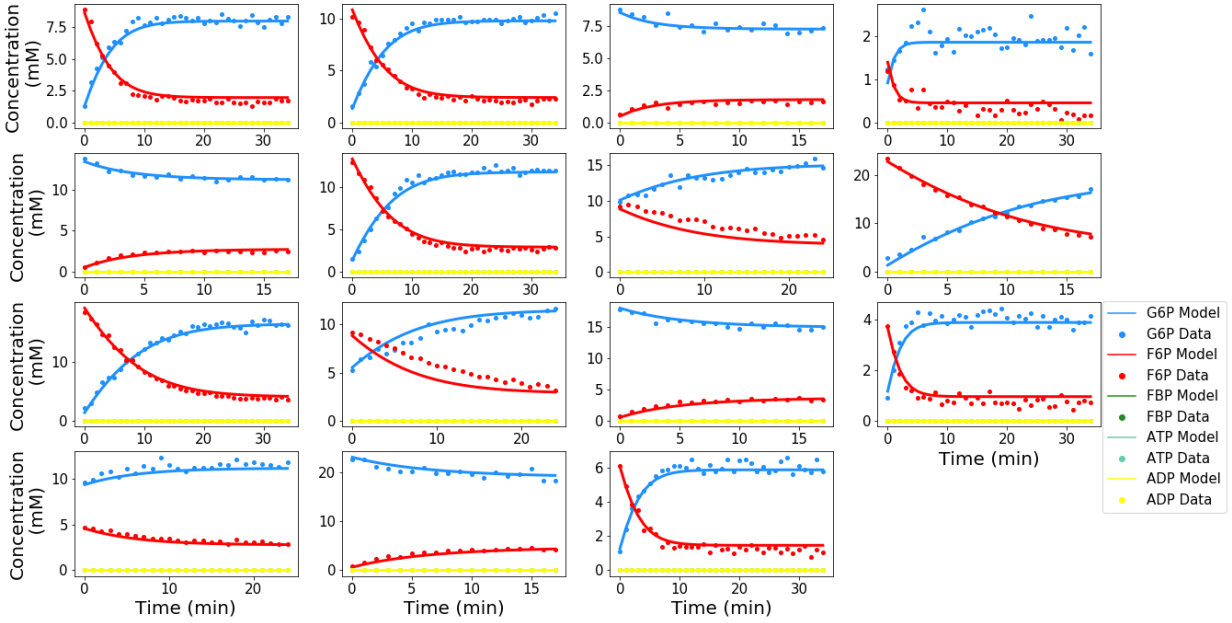

Figure 4.5: Time course data captured for the PGI-PFK catalyzed coupled module at various initial concentrations using a "crowded" solution with 10% (m/v) Ficoll 70. The dotted lines represent experimental NMR data. Solid lines represent a global fit to all the data.

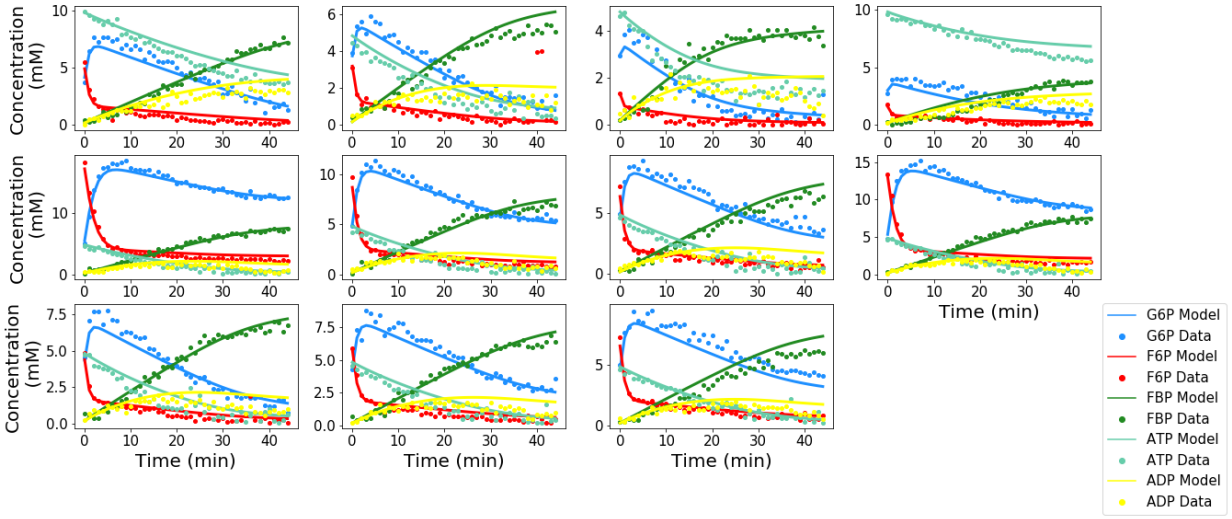

Figure 4.6: Time course data captured for the PGI catalyzed reaction at various initial concentrations using a "crowded" solution with 20% (m/v) Ficoll 70. The dotted lines represent experimental NMR data. Solid lines represent a global fit to all the data.

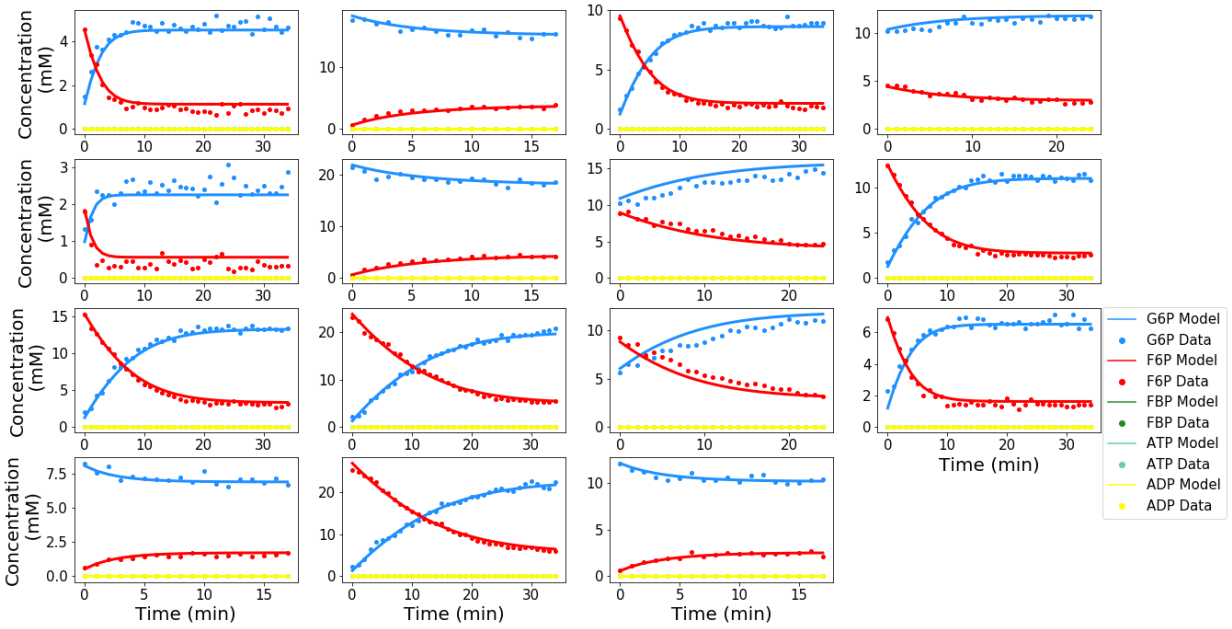

Figure 4.7: Time course data captured for the PGI-PFK catalyzed coupled module at various initial concentrations using a "crowded" solution with 20% (m/v) Ficoll 70. The dotted lines represent experimental NMR data. Solid lines represent a global fit to all the data.

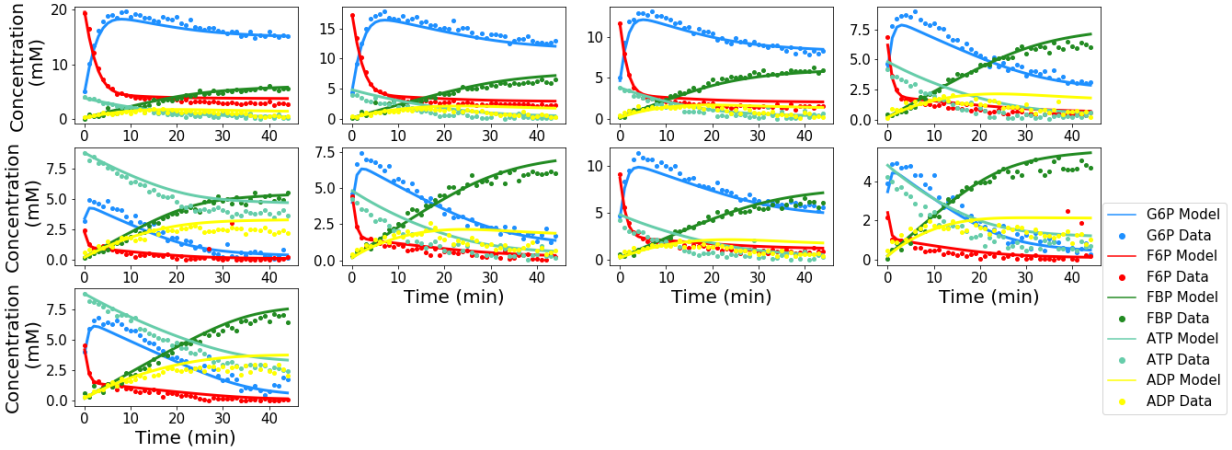

Figure 4.8: Time course data captured for the PGI catalyzed reaction at various initial concentrations using a "crowded" solution with 10% (m/v) PEG 8000. The dotted lines represent experimental NMR data. Solid lines represent a global fit to all the data.

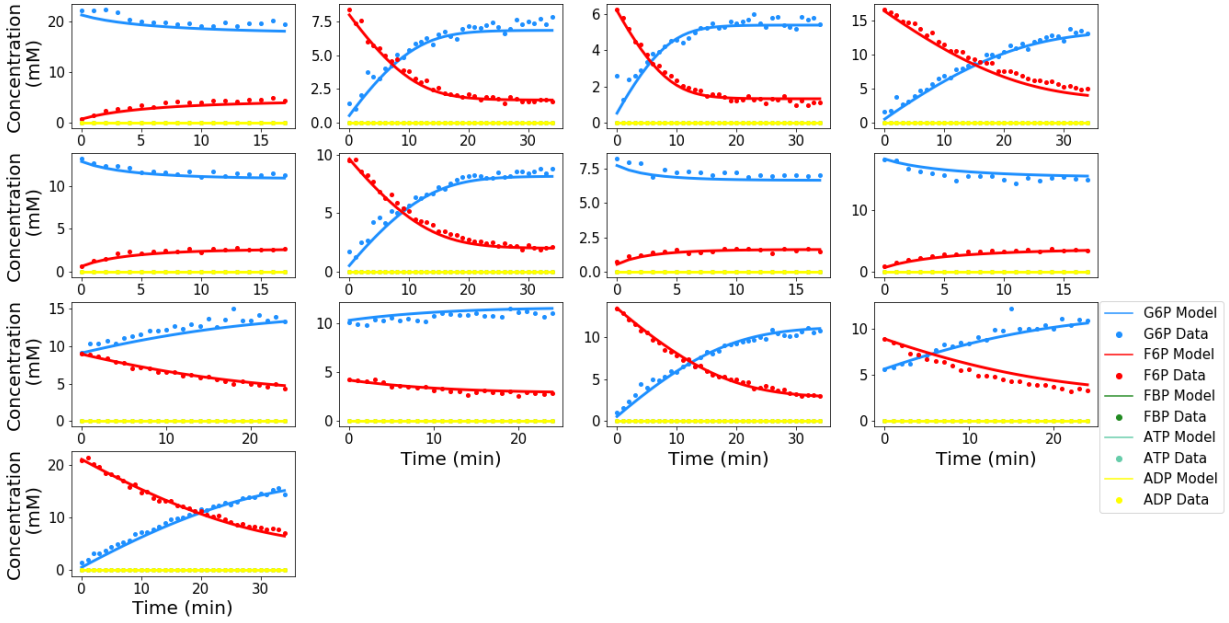

Figure 4.9: Time course data captured for the PGI-PFK catalyzed coupled module at various initial concentrations using a "crowded" solution with 10% (m/v) PEG 8000. The dotted lines represent experimental NMR data. Solid lines represent a global fit to all the data.

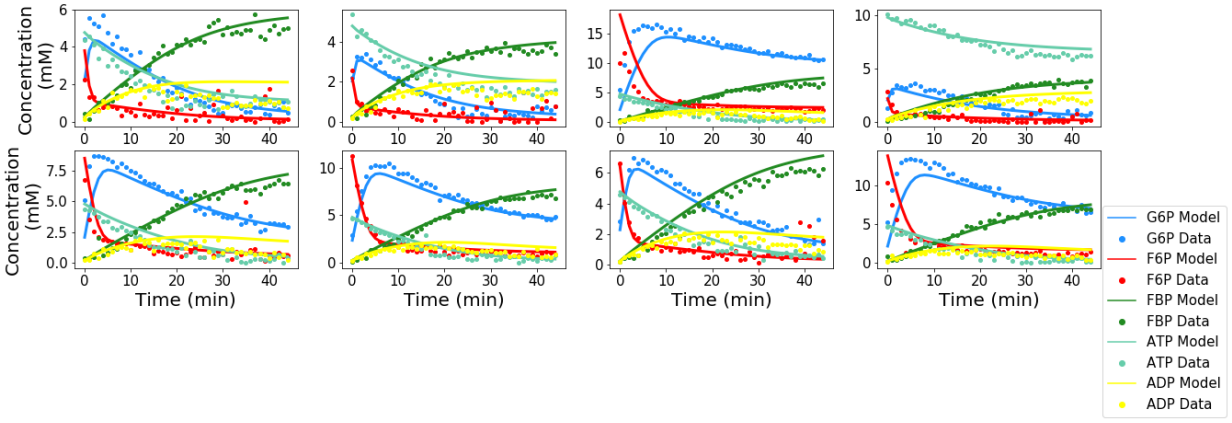

Figure 4.10: Time course data captured for the PGI catalyzed reaction at various initial concentrations using a "crowded" solution with 20% (m/v) PEG 8000. The dotted lines represent experimental NMR data. Solid lines represent a global fit to all the data.

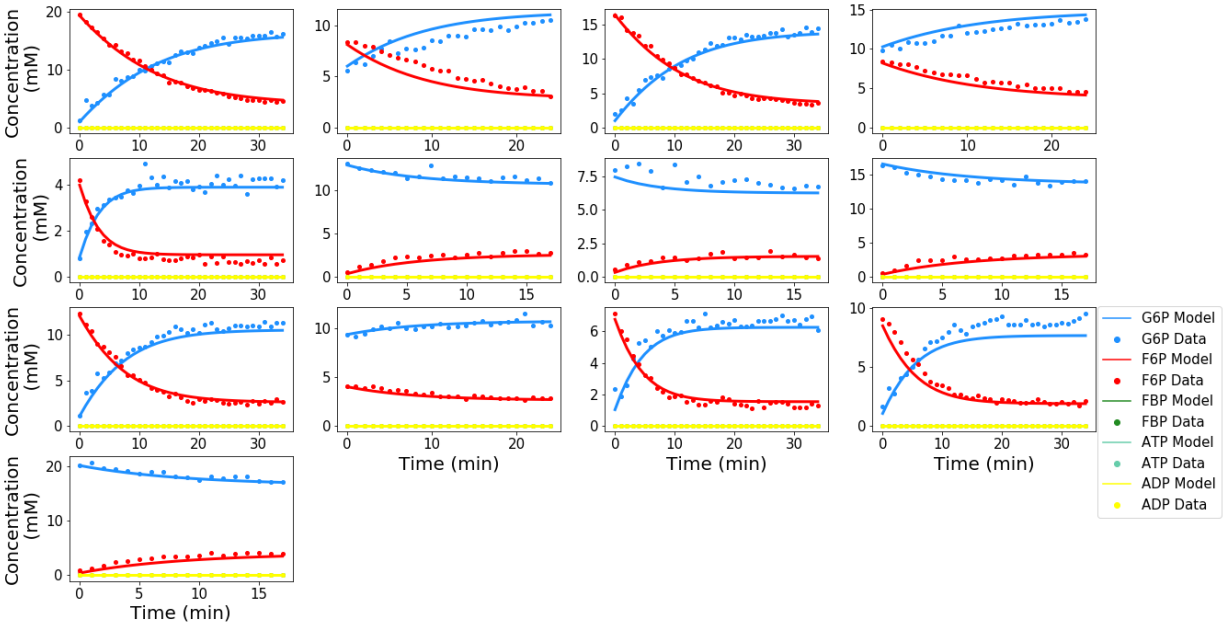

Figure 4.11: Time course data captured for the PGI-PFK catalyzed coupled module at various initial concentrations using a "crowded" solution with 20% (m/v) PEG 8000. The dotted lines represent experimental NMR data. Solid lines represent a global fit to all the data.

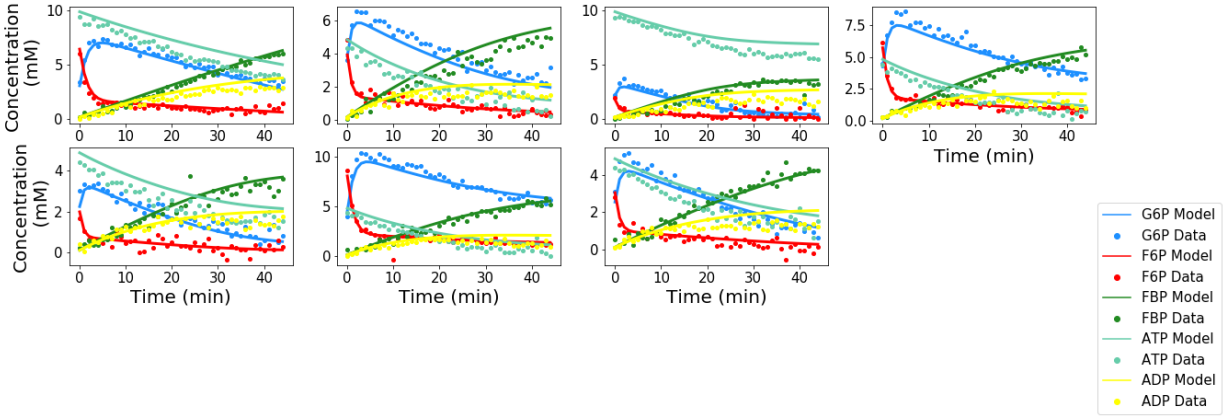

Figure 4.12: Profile likelihood plots of the PGI (a) and PFK (b) kinetic reaction parameters in reference solution. The red dashed line represents the threshold to determine the 95% confidence intervals. The points where the likelihood plot crosses the threshold are the bounds of the 95% confidence intervals.

(a)

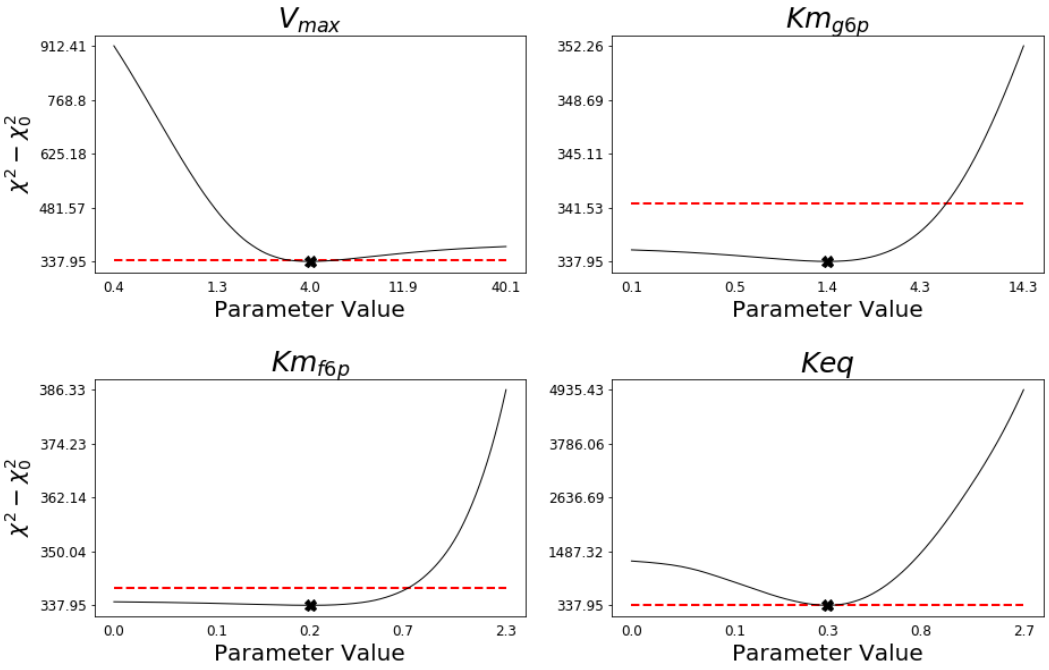

(b)

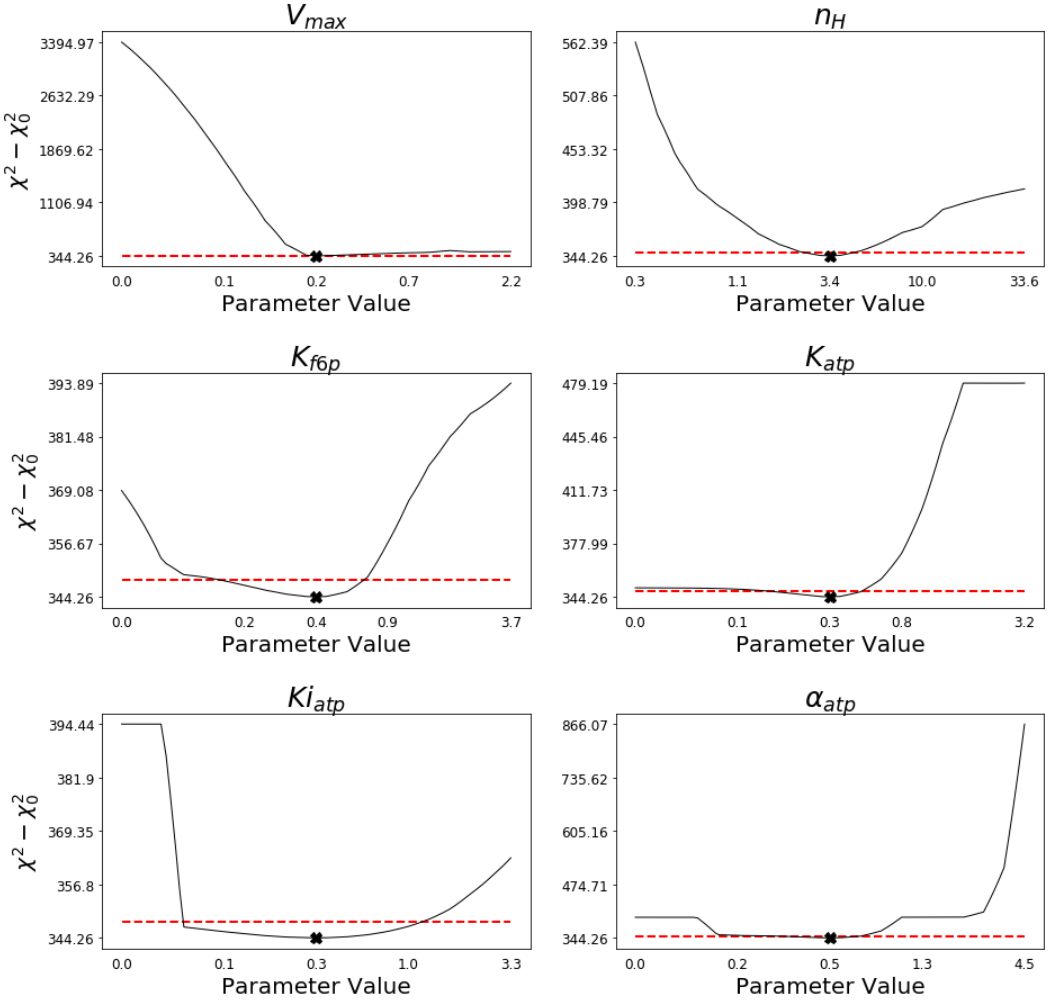

Figure 4.13: Profile likelihood plots of the PGI (a) and PFK (b) kinetic reaction parameters in buffer solution containing 10% (m/v) Ficoll 70. The red dashed line represents the threshold to determine the 95% confidence intervals. The points where the likelihood plot crosses the threshold are the bounds of the 95% confidence intervals.

(a)

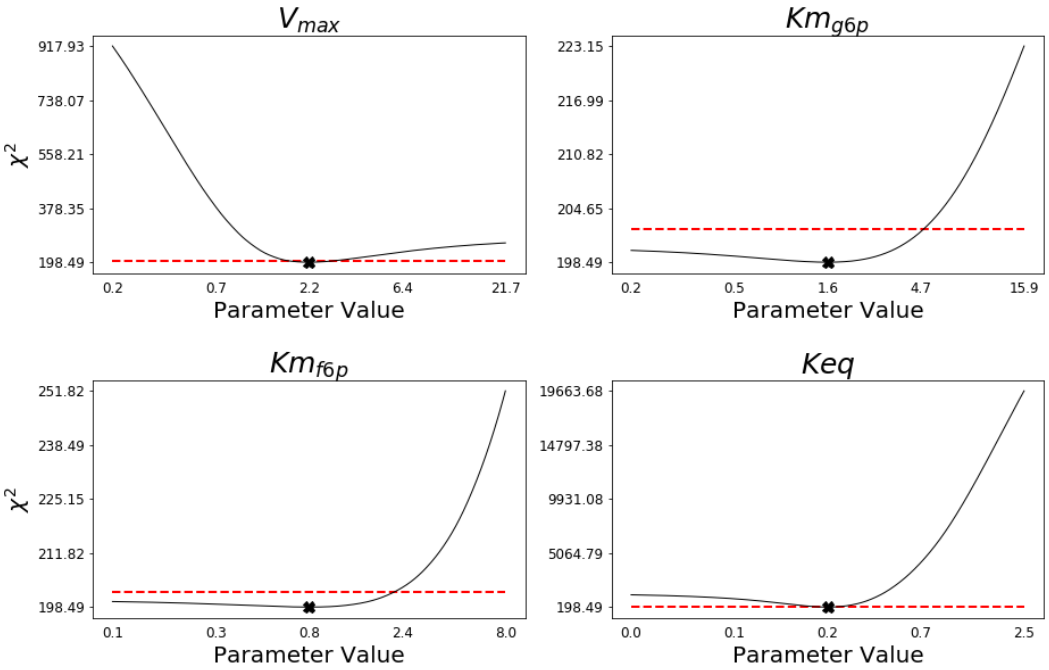

(b)

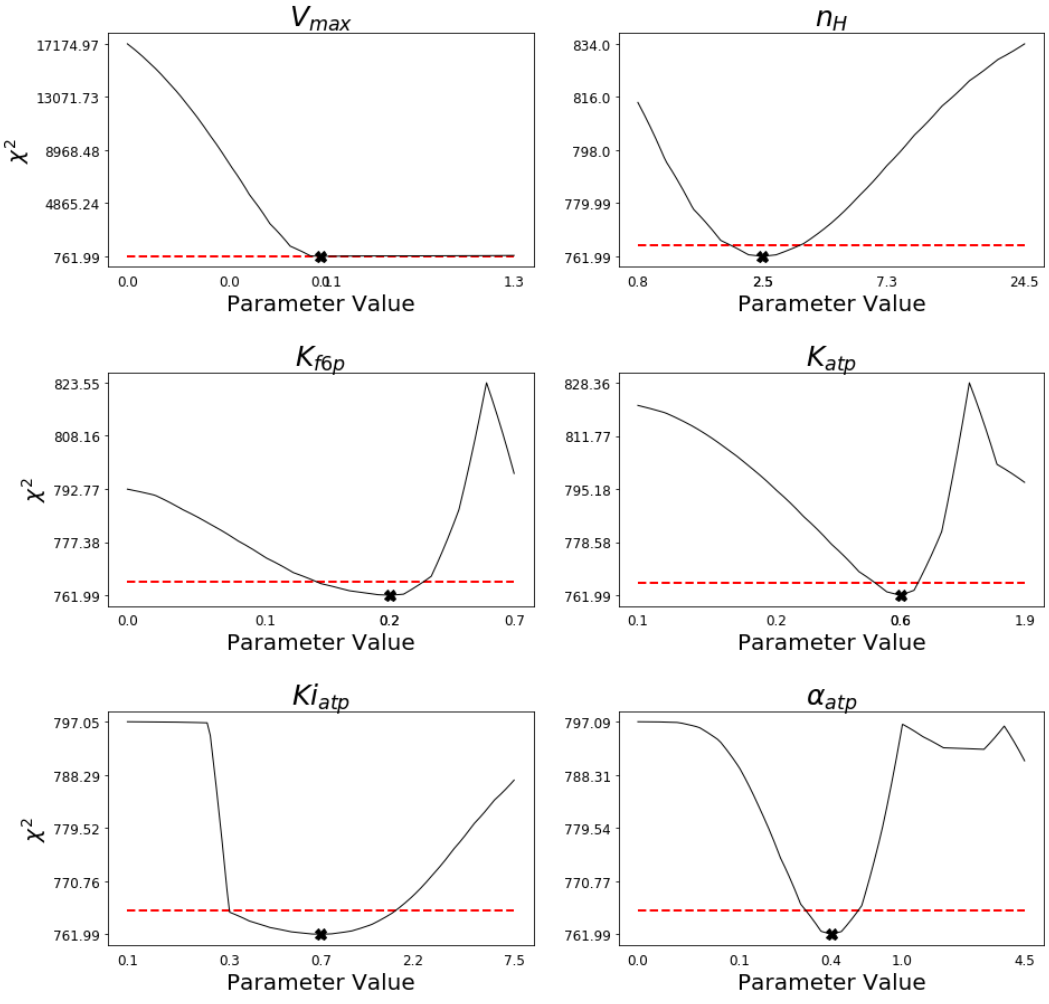

Figure 4.14: Profile likelihood plots of the PGI (a) and PFK (b) kinetic reaction parameters in buffer solution containing 20% (m/v) Ficoll 70. The red dashed line represents the threshold to determine the 95% confidence intervals. The points where the likelihood plot crosses the threshold are the bounds of the 95% confidence intervals.

(a)

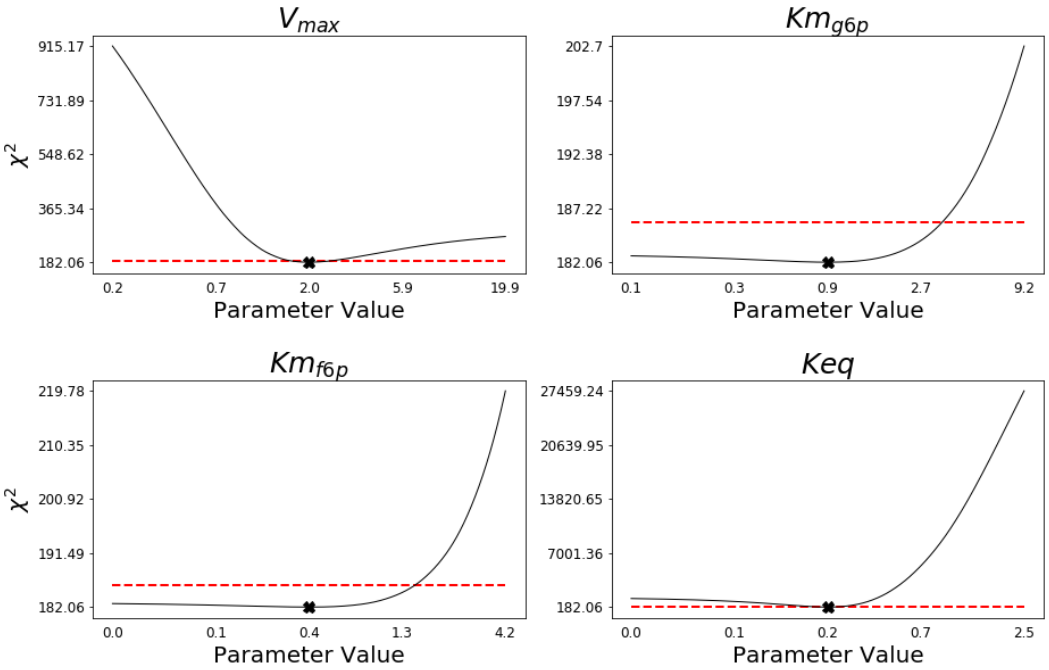

(b)

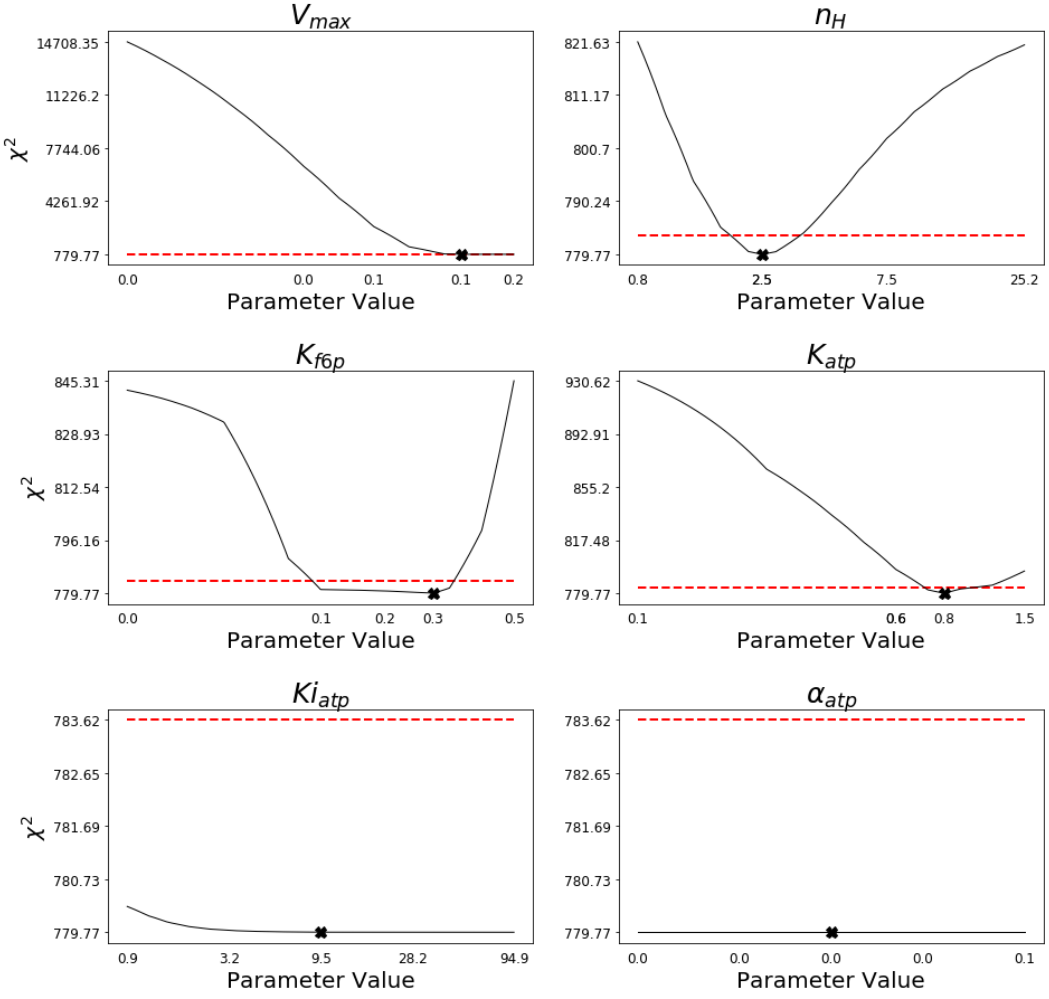

Figure 4.15: Profile likelihood plots of the PGI (a) and PFK (b) kinetic reaction parameters in buffer solution containing 10% (m/v) PEG 8000. The red dashed line represents the threshold to determine the 95% confidence intervals. The points where the likelihood plot crosses the threshold are the bounds of the 95% confidence intervals.

(a)

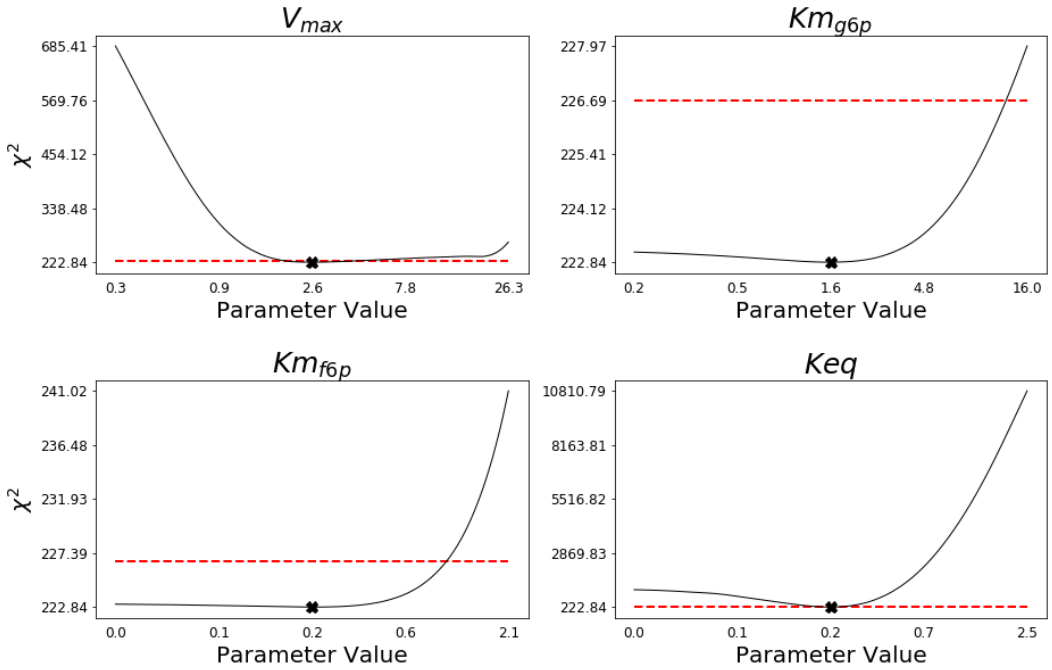

(b)

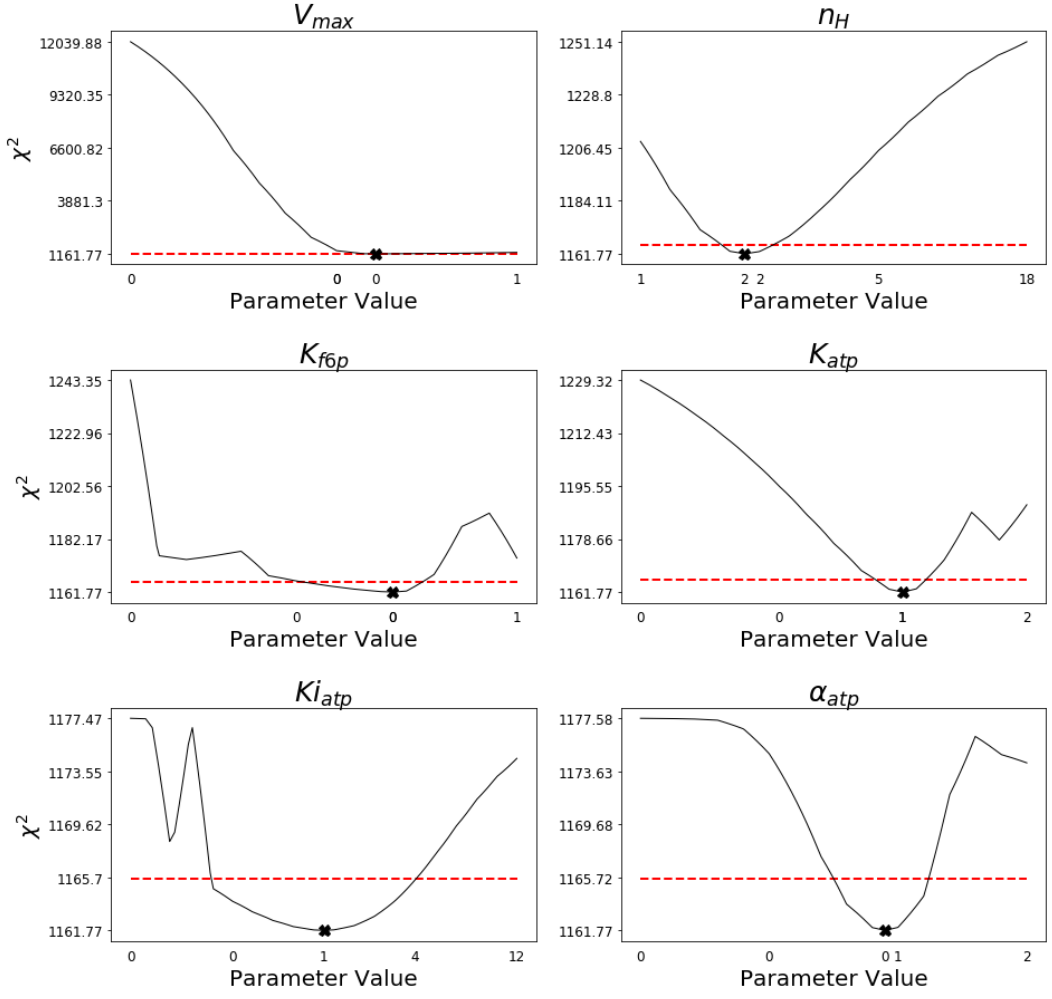

Figure 4.16: Profile likelihood plots of the PGI (a) and PFK (b) kinetic reaction parameters in buffer solution containing 20% (m/v) PEG 8000. The red dashed line represents the threshold to determine the 95% confidence intervals. The points where the likelihood plot crosses the threshold are the bounds of the 95% confidence intervals.

(a)

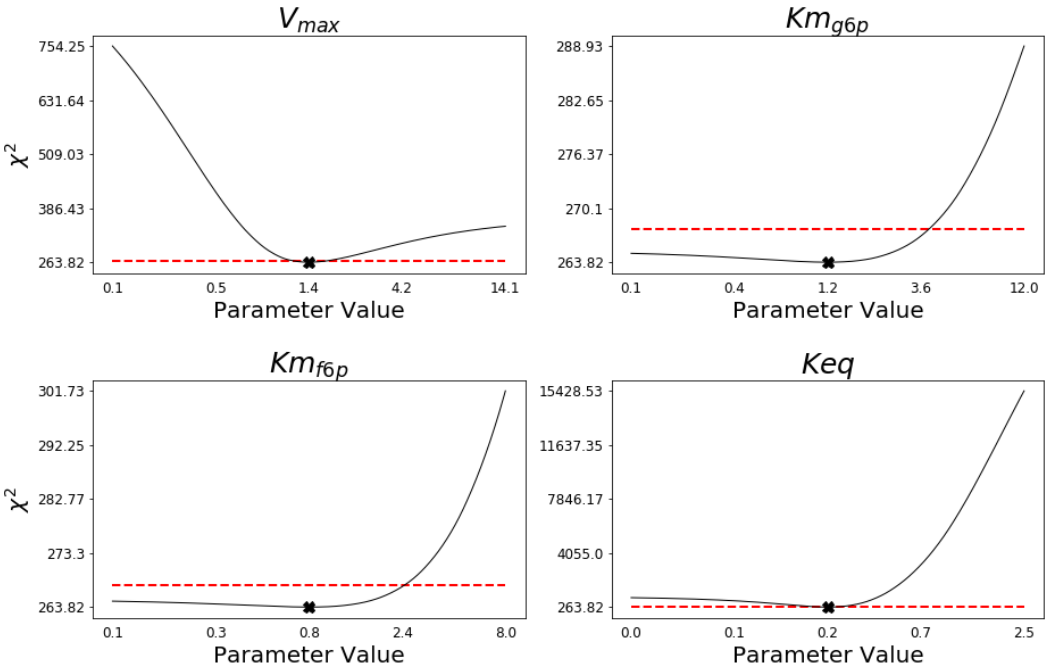

(b)

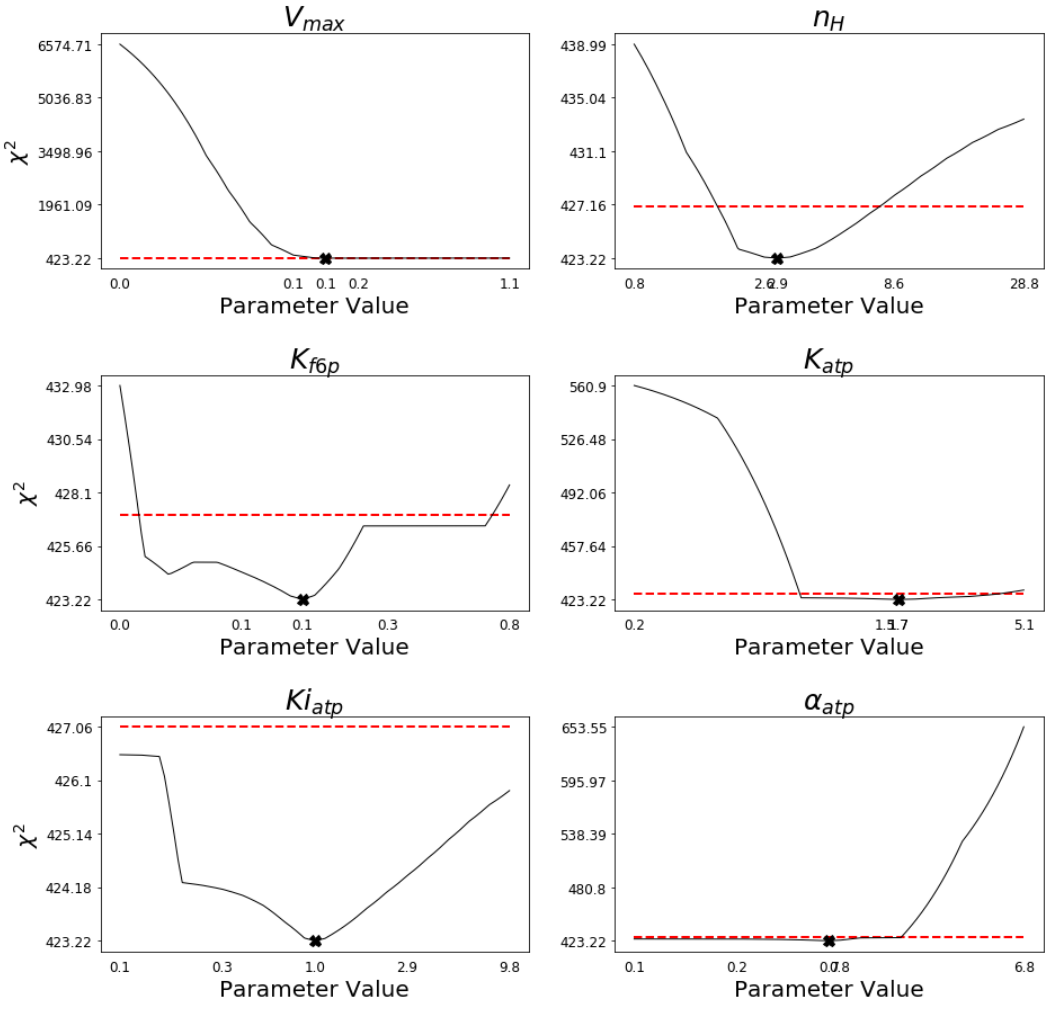

4.2 Identifiability analysis

After the model data was fitted to the gathered ^{31P}NMR data, the parameter estimates were returned and the identifiability of each parameter was assessed to determine the 95% confidence intervals for each (Figures 4.12 - 4.16).
The 95% confidence interval indicates that there is a 95% certainty that the actual value falls between the two values. This was important for the quantification of parameters as we were able to provide statistical estimates of the accuracy of the parameter value. This was explained in detail in Section 2.2.4.

The confidence intervals for a parameter were established by changing the value of the parameter and then keeping it fixed while re-fitting other parameters in the model. The goodness-of-fit-statistic, χ^2, will then change if the other parameters in the model are not able to compensate for the change in the fixed parameter [13]. This was repeated changing the value of the parameter being fixed each time. When the difference between the new χ^2 value and the original value surpasses the threshold value it indicates a bound of the confidence interval. This was done for both increasing and decreasing values to obtain upper an lower confidence intervals.

For all parameters a unique minimum value was determined and they were therefore structurally identifiable. The half-saturation constant parameters for G6P and F6P in the PGI rate reaction were both determined to be practically non-identifiable parameters and only upper confidence regions could be determined for each. The half-saturation constant for ATP as an allosteric modifier and the interaction factor α were determined to be practically non-identifiable in solutions with higher concentrations of either crowding agent, however no confidence intervals could be determined for these, except for the α parameter in buffer solution containing 20% PEG 8000. Figures 4.12 to 4.16 show the identifiability plots for all parameters in all buffer conditions.

The confidence interval of each parameter gives an indication of the margin of error of the relevant parameter. It is an indication of the uncertainty around the point that has been fitted. Therefore, narrower confidence intervals are an indication of a more precise measurement [87]. A confidence interval of 95% indicates a range of values of which we are 95% sure contain the fitted value [88]. Two values can be assumed to be statistically different if their confidence intervals do not overlap [87].

4.3 Fitted parameter values

Phosphoglucose Isomerase

The fitted parameter values for the PGI catalyzed reaction in reference conditions were similar to those in literature. Of the four parameters used to fit the model, only the V_{max} and Keq parameters were both structurally and practically identifiable as described in Section 2.2.4, while both the Km_{f6p} and Km_{g6p} parameters were practically non-identifiable. The practical non-identifiability of these parameters may be

Table 4.1: Fitted parameters for PGI reaction under reference conditions with upper and lower bounds for the 95% confidence intervals. Relevant literature values are also shown for comparison.

Parameter	Lower Bound	Fitted Value	Upper Bound	Literature Value
$V_{max}(\mu\text{mol} \cdot \text{min}^{-1} \cdot \text{mg protein}^{-1})$	3.301	4.009	5.526	
Km_{f6p}(mM)	$-\infty$	0.227	0.712	0.3 [84]
Km_{g6p}(mM)	$-\infty$	1.432	5.764	1.4 [84]
Keq	0.257	0.267	0.278	0.314 [84], 0.23 [89]

solved with further experiments or collection of data with less noise.

The commonly used crowding agents Ficoll 70 and PEG 8000 were used in this study to emulate an increasingly "crowded" cellular environment. They are inert polymers and do not interfere with the reactions directly and any changes observed on parameters can thus be explained by the "crowded" nature of the buffer and, therefore, by the excluded volume effect. A list of all fitted parameter values for the PGI catalyzed reaction in buffer consisting of 10 and 20% (m/v) of either Ficoll 70 or PEG 8000 can be found in Tables 4.1 and 4.2.

As the concentration of crowding agents used in the buffer increased the most drastic changes were observed in the maximum rate (V_{max}) of the PGI reaction. In buffer solution containing 10% crowding agent, the fitted value for V_{max} halved regardless of crowding agent used.

In buffer containing 20% Ficoll 70 the fitted value for V_{max} was similar to the fitted value obtained in solution containing 10% Ficoll 70. In solution containing 20% PEG 8000 the fitted value was slightly lower than the fitted value determined in solution containing 10% PEG 8000 (Figure 4.17 a).

A crowding agent concentration as low as 10% had a major effect of the maximum rate of the reaction. This would suggest that the maximum rate of the PGI reaction was significantly affected in a "crowded" environment, but that this relationship is not linear with the increase in concentration of said crowding agents as the maximum rate only decreased slightly at 20% from the value at 10% for the tested crowding agents. This decrease as the concentration of crowding agent increased was slightly greater in buffer containing the crowding agent PEG 8000.

The half-saturation constant for the substrate, G6P (Km_{g6p}), was determined to be practically non-identifiable and only an upper bound confidence interval could be determined. There was no clear difference between the fitted parameter in solutions containing either 10% Ficoll 70 or 10% PEG 8000 and the reference solution. In

Table 4.2: Fitted parameters for PGI reaction in buffer containing various initial concentrations of Ficoll and PEG

Crowding Agent	Parameter	Lower Bound	Fitted Value	Upper Bound
10% Ficoll 70	$V_{max}(\mu\text{mol} \cdot \text{min}^{-1} \cdot \text{mg protein}^{-1})$	1.827	2.166	2.771
	Km_{f6p}(mM)	$-\infty$	0.804	2.192
	Km_{g6p}(mM)	$-\infty$	1.592	4.923
	Keq	0.246	0.248	0.251
20% Ficoll 70	$V_{max}(\mu\text{mol} \cdot \text{min}^{-1} \cdot \text{mg protein}^{-1})$	1.714	1.986	2.442
	Km_{f6p}(mM)	$-\infty$	0.421	1.444
	Km_{g6p}(mM)	$-\infty$	0.922	3.543
	Keq	0.240	0.249	0.262
10% PEG 8000	$V_{max}(\mu\text{mol} \cdot \text{min}^{-1} \cdot \text{mg protein}^{-1})$	1.908	2.633	4.909
	Km_{f6p}(mM)	$-\infty$	0.211	1.020
	Km_{g6p}(mM)	$-\infty$	1.600	12.515
	Keq	0.239	0.246	0.251
20% PEG 8000	$V_{max}(\mu\text{mol} \cdot \text{min}^{-1} \cdot \text{mg protein}^{-1})$	1.203	1.410	1.748
	Km_{f6p}(mM)	$-\infty$	0.803	2.445
	Km_{g6p}(mM)	$-\infty$	1.197	3.904
	Keq	0.243	0.247	0.253

Table 4.3: Fitted parameters for PFK reaction with no crowding agents

Parameter	Lower Bound	Fitted Value	Upper Bound	Literature Value
$V_{max}(\mu\text{mol} \cdot \text{min}^{-1} \cdot \text{mg protein}^{-1})$	0.212	0.220	0.252	
n_H	2.436	3.363	4.535	2.8 [90]
K_{f6p}(mM)	0.120	0.366	0.638	0.1 [84]
K_{atp}(mM)	0.150	0.322	0.473	0.65[84]
Ki_{atp}(mM)	0.069	0.329	1.164	
α	0.259	0.451	0.635	

buffer solution containing 20% crowding agent, the fitted half-saturation constant parameter and again appeared to remain unchanged (Figure 4.17 b).

The fitted value for the half saturation concentration of F6P was found to be practically non-identifiable in all solutions and only an upper bound confidence interval was determined. In buffer containing 10% Ficoll 70 the fitted parameter increased, but stayed relatively unchanged at in buffer containing 10% PEG 8000. In buffer containing 20% Ficoll 70, the fitted half-saturation constant for F6P was lower than in solution containing 10% Ficoll 70, but was still greater than reference solution. In solution containing 20% PEG 8000 the fitted parameter was greater than in reference solution and 10% PEG 8000. No clear relationship between the half saturation constant for F6P and the concentration of crowding agent present in solution could be established. However, as the parameter was determined to be practically non-identifiable and does not have confidence intervals in both directions it is difficult to make accurate conclusions (Figure 4.17 c).

There appeared to be an initial decrease in the equilibrium constant from an uncrowded buffer to one containing 10% Ficoll 70, but no change from 10% to 20% Ficoll 70. The Keq parameter in uncrowded buffer was fitted at 0.267. In solutions containing 10% or 20% crowding agent, the fitted Keq parameter remained virtually unchanged (Figure 4.17 d). This was to be expected as the relatively small size of both the product and substrate compared to the crowding agents means that these molecules were not affected by the steric repulsion. The equilibrium constant is the ratio of product to substrate at equilibrium and was therefore not expected to change in a "crowded" environment.

Phosphofructosekinase

Here we present a summary of the fitted parameters for the PFK reaction under different crowding agent conditions.

Figure 4.17: Fitted values for the parameters of the PGI catalyzed reaction in buffers containing various initial concentrations of Ficoll 70 and PEG 8000. The parameter values of the reaction in reference conditions are represented in blue. The black error bars represent the range of the 95% confidence intervals. Parameter values which are fully identifiable are shown in red. Parameters which are non-identifiable are shown in light grey and only the upper confidence interval is shown. (a) Maximum rate of reaction (V_{max}); (b) G6P half-saturation constant (Km_{g6p}); (c) F6P half-saturation constant (Km_{f6p}); (d) Equilibrium constant (Keq).

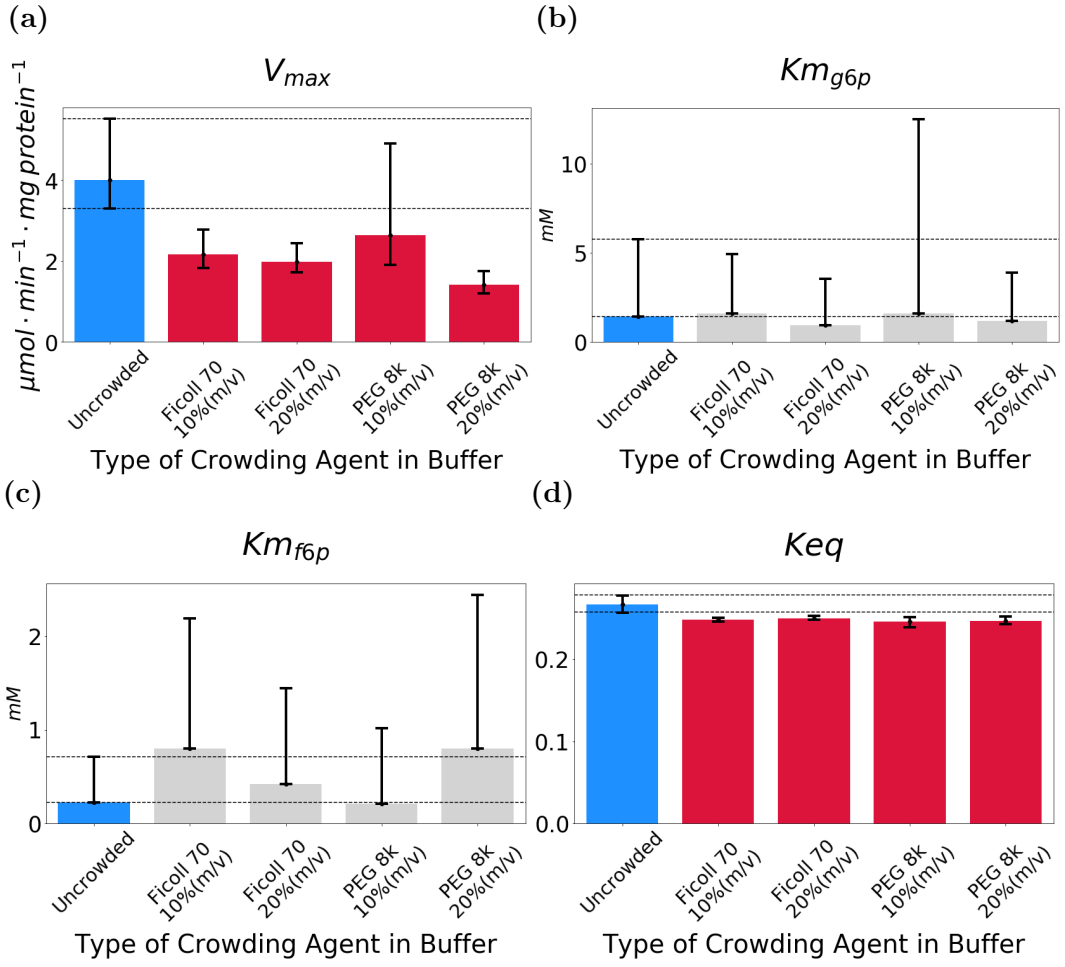

Table 4.4: Fitted parameters for PFK reaction in buffer containing 10% and 20% (m/v) Ficoll 70 and PEG 8000

Crowding Agent	Parameter	Lower Bound	Fitted Value	Upper Bound
10% Ficoll 70	$V_{max}(\mu\text{mol} \cdot \text{min}^{-1} \cdot \text{mg protein}^{-1})$	0.130	0.131	0.142
	n_H	1.868	2.453	3.411
	K_{f6p}(mM)	0.124	0.233	0.312
	K_{atp}(mM)	0.501	0.622	0.724
	Ki_{atp}(mM)	0.252	0.746	1.805
	α	0.331	0.445	0.610
20% Ficoll 70	$V_{max}(\mu\text{mol} \cdot \text{min}^{-1} \cdot \text{mg protein}^{-1})$	0.127	0.129	0.186
	n_H	1.921	2.522	3.531
	K_{f6p}(mM)	0.108	0.267	4.923
	K_{atp}(mM)	0.727	0.837	1.018
	Ki_{atp}(mM)	$-\infty$	9.488	∞
	α	$-\infty$	0.007	∞
10% PEG 8000	$V_{max}(\mu\text{mol} \cdot \text{min}^{-1} \cdot \text{mg protein}^{-1})$	0.130	0.140	0.164
	n_H	1.518	1.828	2.307
	K_{f6p}(mM)	0.142	0.307	0.397
	K_{atp}(mM)	0.611	0.770	0.942
	Ki_{atp}(mM)	0.331	1.232	3.712
	α	0.304	0.492	0.741
20% PEG 8000	$V_{max}(\mu\text{mol} \cdot \text{min}^{-1} \cdot \text{mg protein}^{-1})$	0.122	0.137	1.073
	n_H	1.670	2.884	7.561
	K_{f6p}(mM)	0.014	0.108	0.711
	$Katp$(mM)	0.729	1.714	4.193
	Ki_{atp}(mM)	$-\infty$	0.978	∞
	α	$-\infty$	0.682	1.597

The fitted V_{max} was lower in solution consisting of either 10% Ficoll 70 or 10% PEG 8000 than in reference solution. In solution containing 20% of either crowding agent, the fitted V_{max} remained virtually unchanged to the value fitted in 10% crowding agent (Figure 4.18 a).

In uncrowded solution the Hill coefficient (n_H) was determined to be 3.363. In solution containing either 10% or 20% Ficoll 70 it was fitted at a slightly lower value, indicating a loss of co-operativity (Figure 4.18 f). A similar trend was observed in solutions containing PEG 8000.

The fitted half-saturation constant for F6P (K_{f6p}) decreased in 10% Ficoll 70 but remained mostly unchanged at solution containing 20% Ficoll 70. In solution containing 10% PEG 8000 the fitted value was lower than the fitted reference value and was decreased even further in solution containig 20% PEG 8000 (Figure 4.18 b). This would suggest that the binding of F6P to PFK is favoured in crowded conditions. Conversely the half-saturation constant for ATP increased as the crowding agent concentration was increased (Figure 4.18 c).

The half-saturation constant for ATP binding to the allosteric site on the PFK enzyme, Ki_{atp}, also increased with the increase in crowding agent concentration. As the crowding agent concentration increased to 20% no confidence intervals, either upper or lower, could be determined for Ki_{atp}, and were determined to be practically non-identifiable, however true minima were determined. (Figure 4.18 d)

The interaction factor α remained virtually unchanged with the addition of 10% crowding agents. It was determined to be 0.451 in reference solution, 0.445 in solution with 10% Ficoll 70, and 0.492 in solution with 10% PEG 8000 (Figure 4.18 e). However, a higher concentration of crowding agents had a more pronounced effect: the fitted parameter value was 0.007 in 20% Ficoll 70 and 0.682 in 20% PEG 8000. The values determined in solutions containing 20% of each of the crowding agents were practically non-identifiable.

In the following chapter we will discuss these results in the context of current literature.

Figure 4.18: Fitted values for the parameters of the PFK catalyzed reaction in buffers containing various initial concentrations of Ficoll 70 and PEG 8000. The parameter values of the reaction in reference conditions are represented in blue. The black error bars represent the range of the 95% confidence intervals. Parameter values which are identifiable are shown in red. Parameters which are non-identifiable are shown in light grey. (a) Maximum rate of reaction (V_{max}); (b) F6P half-saturation constant (K_{f6p}); (c) ATP half-saturation constant (K_{atp}); (d) Allosteric modifier half-saturation constant (Ki_{atp}); (e) Interaction factor α; and (f) Hill coefficient (n_H)

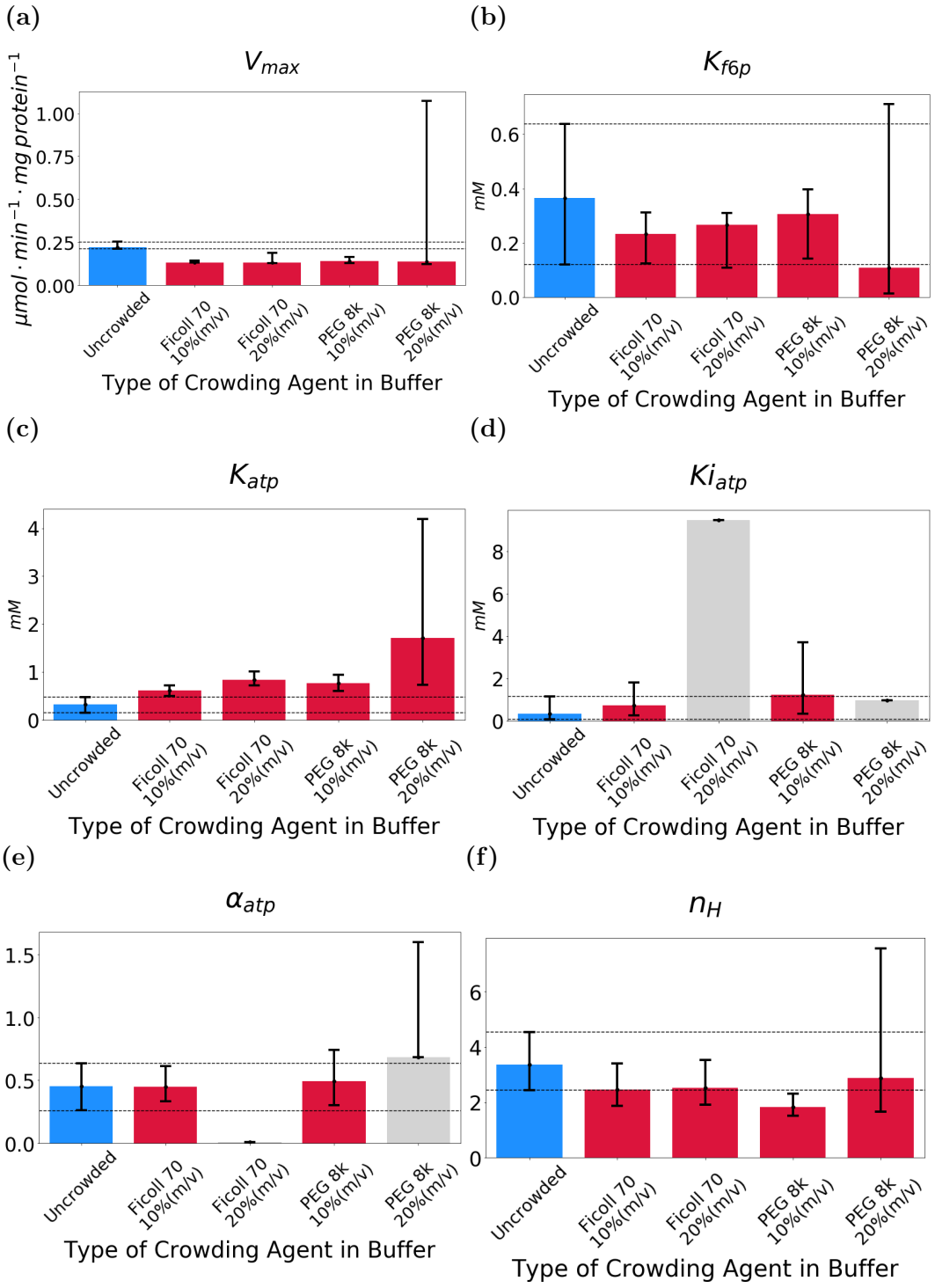

Chapter 5

Discussion

The results presented in Chapter 4 are discussed here in relation to the set of objectives laid out in Chapter 1. Suggestions for future studies will also be discussed here.

The aim of this study was to determine the effects of macromolecular crowding on the enzyme kinetics of the upper glycolytic enzymes phosphoglucose isomerase (PGI) and phosphofructokinase (PFK) and aid in the creation of a set of standard assay conditions which are representative of *in vivo* conditions, namely by determining whether the macromolecular crowding phenomenon should be taken into account in the definition of these standardized assay conditions.

5.1 Synopsis

In this study NMR time-course assays were performed and the data fitted to a kinetic model to determine parameter values. The accuracy and identifiability of each parameter was investigated by exploring the profile-likelihoods of each parameter [13]. After this analysis it was observed that macromolecular crowding had the greatest affect on the maximum rate of both PGI and PFK. The maximum rate of both enzymes decreased in the presence of crowding agents. The half-saturation constant for F6P in the PFK reaction decreased in the presence of crowding agents and the half-saturation constant for ATP increased. Other parameter changes were either not significant or involved parameters which were non-identifiable. In this chapter the identifiability of parameters will be discussed and solutions given to resolve non-identifiability. Possible reasons for the observed changes in "crowded" conditions are also explored, and its inclusion in a standardized solution for studying enzyme kinetics is also discussed. Suggestions for future work are also included.

5.2 Identifiability of parameters

The identifiability analysis was done by exploiting the profile likelihood of each parameter, as was explained in Section 2.2.4. An identifiable parameter is one with finite confidence intervals which represent the upper and lower bounds of the 95% confidence regions. Narrow confidence intervals are an indication of the accuracy of

the fitted parameter value. Non-identifiability of a parameter can either be structural or practical. Structural non-identifiability is the result of redundant parameters in the model and changes to structurally non-identifiable parameters can be fully compensated by other parameters in the model and no change in the χ^2 is observed [13]. This manifests as a completely flat valley in the profile-likelihood. Practical non-identifiability results from poor or insufficient data. Unique minima are found, but at least one confidence interval does not cross the threshold [13]. This is discussed further in Section 2.2.4.

The profile likelihood plots for all parameters are shown in Figures 4.12 to 4.16. In all of the buffer conditions V_{max} and K_{eq} were found to be identifiable while K_{g6p} and K_{f6p} were found to be practically non-identifiable. The NMR technique used in this study was not sensitive enough to accurately determine low metabolite concentrations. For the parameters of the PFK model in buffers with 10% crowding agents (Ficoll 70 and PEG 8000) all of the parameters were found to be identifiable and finite confidence intervals could be determined for all of them. In buffers containing 20% crowding agents the parameters for the affinity of ATP for the regulatory site on PFK (Ki_{atp}) and α were found to be practically non-identifiable as at the higher concentrations of crowding agents the quality of data decreased. In buffer containing 20% Ficoll the α parameter could be mistaken for being structurally non-identifiable since it is a flat valley with no minimum. However, structural non-identifiability arises from redundant parameterization and is a property of the model [13]. Since in all other buffer conditions a minimum could be determined it cannot be structurally non-identifiable but rather practically non-identifiable.

From the identifiability analysis it can be seen that more data would need to be collected for the buffer conditions containing 20% PEG and Ficoll in order to solve the practical non-identifiability of the PFK parameters. However for all of the parameters unique minima could be found making it possible to draw some conclusions.

5.3 The effects of macromolecular crowding on kinetic parameters

Macromolecular crowding is an ubiquitous phenomenon in the intracellular environment, but is often neglected when developing experiments to mimic *in vivo* conditions. It has been a known property of the intracellular environment for many years [8], but is mostly ignored as traditionally enzyme kinetic assays have been performed in ideal solutions with minimum amounts of macromolecules [5]. This is mostly done as a matter of convenience as adding large quantities of macromolecules to the buffer can make it viscous and difficult to work with, which may compromise accuracy [2]. There have been numerous studies on the effects of macromolecular crowding on the kinetic parameters of an enzyme [20; 54–58]. These studies focus on enzymes that follow traditional Michaelis-Menten kinetics as these are easy to assay and the kinetics are well understood. In this study we focused on the two upper glycolytic enzymes: PGI and PFK.

5.3.1 Phosphoglucose isomerase

PGI is a dimeric enzyme consisting of two identical monomers which catalyzes the second step in the glycolytic pathway and is responsible for the interconversion of glucose-6-phosphate (G6P) to fructose-6-phosphate (F6P) and the opposite reaction in gluconeogenesis [91]. This is done via hydrogen transfer using an enediol intermediate [92]. The two monomers both contain active sites, however, the dimerization of the protein is critical for enzyme activity [93].

Our results show that there was a significant decrease in the V_{max} of the reaction in the crowded buffers compared to the uncrowded buffer (Tables 4.1 and 4.2). This is in agreement with other observations made by others with reactions which follow Michaelis-Menten kinetics [54–56]. As discussed in Section 2.1.6 it is the dimerization of the protein which is favoured in a crowded environment due to the reduction of entropy in the system. It may be expected that this would lead to an increase in the enzyme activity of the reaction as the active dimer form is favoured but the observed decrease is most probably due to the increase in viscosity of the buffer due to the large amount of macromolecules, causing decreased diffusion compared to an ideal solution resulting in the reduction of the number of interactions between the substrate and the enzyme and therefore a decrease in enzyme activity. The V_{max} for the reaction in buffer containing 10% (w/v) PEG was the only value which was not found to be significantly changed as the range of its confidence intervals overlapped with those of the uncrowded parameter. It also had a larger confidence interval than was found in other buffers. The large confidence interval range can be reduced with the acquisition of additional, more precise data.

For the half-saturation constant for G6P (K_{g6p}) and F6P (K_{f6p}) the fitted parameters were near the expected literature values [84]. Although minimum values were found for all K_m values for both G6P and F6P in all buffer conditions, they were all found to be practically non-identifiable. There appears to be no difference in the K_{g6p} parameter between the non-crowded and crowded conditions suggesting that the affinity of PGI for G6P remains unchanged regardless of the amount of crowding agents present in the buffer. Interestingly, the fitted parameter for the half-saturation constant for F6P appears to slightly increase in crowded environments, indicating that F6P binds less favourably to the enzyme in crowded environments. It is unlikely that this change in the affinity of PGI for F6P is due to slower molecular diffusion as has been suggested in other studies [55; 57] as G6P and F6P are very similar molecules and it is unlikely that the change in diffusion would only affect the one and not the other. It is most likely due to slight conformational changes of PGI in a crowded environment.

The fitted parameter for the equilibrium constant (K_{eq}) in the uncrowded buffer was similar to what has been reported in literature [84; 89]. It was expected that there would be little to no change in the parameter in the crowded buffers compared to the uncrowded buffer as the relatively small size of the substrate and product means that the excluded volume should have little to no effect [55]. Our results showed that the K_{eq} decreased slightly in the presence of a highly crowded environment. However

these changes still fall within what would be expected from literature values.

5.3.2 Phosphofructokinase

PFK is the third enzyme in the glycolytic pathway and catalyzes an ATP-dependant reaction that phosphorylates F6P to form fructose 1,6-bisphosphate (FBP). It is a highly regulated enzyme and in eukaryotes is affected by at least 20 different compounds [94]. In yeast the PFK enzyme is a hetero-octameric enzyme composed of 4 α- and 4 β-subunits [95]. This is different to bacterial organisms such as *Escherichia coli* where the enzyme is expressed as homotetramers. Where PFK in *Escherichia coli* is described as a dimer of dimers, the PFK enzyme in *Saccharomyces cerevisiae* has been described as a dimer of tetramers [96]. The PFK in *Saccharomyces cerevisiae* is double the size of its bacterial counterparts and has twice the number of active sites. PFK shows cooperative binding for F6P, while ATP acts as an inhibitor [90], and exists in either an active R-state or an inactive T-state. The change from T- to R-state is induced by the binding of F6P to the enzyme [97].

As described in Section 3.4 the PFK reaction was modelled using an irreversible bi-bi Hill equation. Using this model we were able to incorporate binding kinetics for the products as well as the allosteric inhibition by ATP. When placed in crowded media the maximum rate of the reaction appeared to decrease for all crowding agents and at all concentrations though this appears to not be dependent on the type nor concentration of the crowding agent in the buffer. As was the case for PGI this is probably due to a combination of conformational changes as the crowded environment favours a more compact form of the protein as well as the slower diffusion may result in fewer interactions between PFK and its substrates.

The half-saturation constants for F6P and ATP (K_{f6p} and K_{atp} respectively) represent the enzyme's affinity for each of the substrates. The affinity of the enzyme for F6P did not appear to change substantially in buffer conditions which contained crowding agents (Table 4.4 and Figure 4.18 b). The PFK affinity for ATP at the active or regulatory site (K_{atp} and Ki_{atp}) in crowded buffers both seemed to decrease (the parameter value increased) (Table 4.4 and Figure 4.18 c and d). In buffers containing either Ficoll or PEG the affinity appears to decrease as the concentration of crowding agents in the buffer increases. This may be due to the enzyme folding into an energetically more favourable shape which is unfavourable for the reaction to be catalysed in the crowded environment [57]. This would make it difficult for the enzyme to undergo the necessary conformational change to associate with ATP lowering the enzyme's affinity for ATP.

The Hill coefficient (n_H) describes binding cooperativity. A Hill coefficient of 1 indicates non-cooperativity [81]. In uncrowded buffer the Hill coefficient was fitted at a value of 3.363 which indicates high cooperativity. In the crowded buffers the cooperativity appears to decrease slightly. This is most probably the result of conformation changes caused by the entropic pressure in the crowded environment.

The α parameter is an indication of the allosteric effects of ATP upon binding to the enzyme. If α is greater than 1 it indicates activation and if α is less than 1 it indicates inhibition. ATP acts as an allosteric inhibitor and this was corroborated by the fitted value in the uncrowded buffer (0.451). In crowded environments the value remained relatively unchanged, indicating that the allosteric effect that ATP has on PFK remains the same. This is to be expected as macromolecular crowding has been shown to change half-saturation constants and maximum rates (summarized in Table 2.1), but not the allosteric effects of ligands. The value fitted for the buffer containing 20% Ficoll was extremely low, however the parameter was found to practically unidentifiable with no confidence intervals indicating that further data collection is needed.

5.4 Standardization of *in vivo* assay conditions

In an attempt to develop a standardized buffer for studying enzyme kinetics that replicates the intracellular environment *in vivo* for *Saccharomyces cerevisiae*, Van Eunen *at al.* [3] found that macromolecular crowding did not have a significant effect on the activity of glycolytic enzymes and concluded that it was not necessary to account for the crowded cytosolic environment. In that study they made use of PEG and BSA to simulate the effects of macromolecular crowding, but do not mention what concentration they used, and furthermore they only investigated the effects on V_{max}. It has been shown that PEG 8000 has an effect on the kinetics of the glycolytic enzymes hexokinase and pyruvate kinase at concentrations of 10% and 30% [98]. Our data are in agreement with this finding and show that even a buffer solution containing 10% PEG or Ficoll has an effect on the enzyme kinetics, which contradicts the results found by Van Eunen *et al.* [3]. We found that macromolecular crowding does have an effect on the enzyme kinetics of PGI and PFK and it should be considered when studying kinetics *in vivo* when trying to replicate intracellular conditions.

Many studies have investigated the effects of macromolecular crowding on a variety of enzyme kinetics with various results (summarized in Section 2.1.6). It has been suggested that the type of crowder used to mimic macromolecular crowding conditions may effect the enzyme kinetics differently [99]. In this study we used two commonly used polymers, PEG 8000 and Ficoll 70, at two different concentrations to mimic macromolecular crowding inside the cell. There was no difference found between the two different crowding agents. For both crowders the trends observed appeared to be very similar. There are some fitted parameters which appear to differ depending on the type of crowder used (such as K_{atp}), however these almost always coincide with either large confidence intervals or non-identifiability and are less accurate, making it difficult to ascertain whether the changes are significant. From our results it seems that the volume occupied by crowding agents is more important than the type of crowder used. Macromolecular crowding appears to affect enzyme kinetics, but as has been mentioned previously, the increased viscosity caused by the large concentration of crowding agents complicates accurate liquid handling in assays [2].

5.5 Future work

From our data it seems clear that the crowded environment can in some cases have a profound effect on the rate kinetics of enzymes and should be taken into account when performing *in vitro* studies that aim to emulate *in vivo* conditions. However there remain other aspects of this topic, which could be explored.

Fixing the practical non-identifiability of parameters and reducing the confidence intervals of parameters which had large confidence intervals by collecting more accurate data, as explained by Raue *et al.* [13], would allow us to make more accurate conclusions on the effect on these parameters by macromolecular crowding. Additionally, extending the experiments to incorporate data at other concentrations of crowding agents, especially those at concentrations closer to what would be expected in the cytosol, would aid in trying to emulate the effects which would be expected in the cell. This may help gain further insight into the effect of macromolecular crowding on enzyme kinetics *in vivo*.

In this study the trends for Ficoll 70 and PEG 8000 were very similar; however, we did not investigate how different sizes (M_r) of the same crowding agent affect enzyme kinetics. Additionally, as the intracellular environment consists of a mixture of various macromolecules, it would be beneficial to see what effects creating a mixture of different crowding agents may have. It has been shown that a combination of crowding agents can accelerate the folding of enzymes [100] and has been shown to induce greater cooperativity in human serum albumin [101]. It seems likely that if a combination of different crowding agents has more pronounced effects on enzyme behaviour, then enzyme kinetics should be studied under these conditions as well. We have shown that enzyme kinetics are affected by macromolecular crowding, however how this will affect an entire model has not yet been explored. It would therefore be beneficial to incorporate the effects of macromolecular crowding into a whole metabolic model, such as the glycolytic model constructed by Teusink *et al.* [84], to observe if there are any effects.

The effects of macromolecular crowding on enzyme kinetics are often overlooked. This is despite it being a property of the crowded environment in which these reactions take place. This study has demonstrated that enzyme kinetics can be affected by macromolecular crowding and that this should be considered when attempting to construct mathematical models that aim to simulate these reactions under *in vivo* conditions.

Bibliography

[1] Westerhoff, H.V., Kolodkin, A., Conradie, R., Wilkinson, S.J., Bruggeman, F.J., Krab, K., van Schuppen, J.H., Hardin, H., Bakker, B.M., Moné, M.J., Rybakova, K.N., Eijken, M., van Leeuwen, H.J. and Snoep, J.L.: Systems biology towards life in silico: Mathematics of the control of living cells. *Journal of Mathematical Biology*, vol. 58, no. 1-2, pp. 7–34, 2009. ISSN 03036812.

[2] van Eunen, K. and Bakker, B.M.: The importance and challenges of in vivo-like enzyme kinetics. *Perspectives in Science*, vol. 1, no. 1-6, pp. 126–130, 2014. ISSN 22130209.

[3] Van Eunen, K., Bouwman, J., Daran-Lapujade, P., Postmus, J., Canelas, A.B., Mensonides, F.I.C., Orij, R., Tuzun, I., Van Den Brink, J., Smits, G.J., Van Gulik, W.M., Brul, S., Heijnen, J.J., De Winde, J.H., Teixeira De Mattos, M.J., Kettner, C., Nielsen, J., Westerhoff, H.V. and Bakker, B.M.: Measuring enzyme activities under standardized in vivo-like conditions for systems biology. *FEBS Journal*, vol. 277, no. 3, pp. 749–760, 2010. ISSN 1742464X.

[4] García-Contreras, R., Vos, P., Westerhoff, H.V. and Boogerd, F.C.: Why in vivo may not equal in vitro - New effectors revealed by measurement of enzymatic activities under the same in vivo-like assay conditions. *FEBS Journal*, vol. 279, no. 22, pp. 4145–4159, 2012. ISSN 1742464X.

[5] Ellis, R.J.: Macromolecular crowding: An important but neglected aspect of the intracellular environment. *Current Opinion in Structural Biology*, vol. 11, no. 1, pp. 114–119, 2001. ISSN 0959440X.

[6] Minton, A.P. and Wilf, J.: Effect of Macromolecular Crowding upon the Structure and Function of an Enzyme: Glyceraldehyde-3-phosphate Dehydrogenase. *Biochemistry*, vol. 20, no. 17, pp. 4821–4826, 1981. ISSN 15204995.

[7] Zhou, H.-X., Rivas, G. and Minton, A.P.: Macromolecular crowding and confinement: biochemical, biophysical, and potential physiological consequences. *Annu Rev Biophys*, vol. 37, pp. 375–397, 2010.

[8] Laurent, T.C.: Enzyme reactions in polymer media. *European journal of biochemistry / FEBS*, vol. 21, no. 4, pp. 498–506, 1971. ISSN 0014-2956.

[9] Goudar, C.T., Harris, S.K., McInerney, M.J. and Suflita, J.M.: Progress curve analysis for enzyme and microbial kinetic reactions using explicit solutions based on the Lambert W function. *Journal of Microbiological Methods*, vol. 59, no. 3, pp. 317–326, 2004. ISSN 01677012.

[10] Johnson, K.A.: A century of enzyme kinetic analysis, 1913 to 2013. *FEBS Letters*, vol. 587, no. 17, pp. 2753–2766, 2013. ISSN 00145793.

[11] Duggleby, R.G.: Analysis of enzyme progress curves by nonlinear regression. *Methods in Enzymology*, vol. 249, no. C, pp. 61–90, 1995. ISSN 15577988.

[12] Eicher, J.J.: *Understanding glycolysis in Escherichia coli : a systems approach using nuclear magnetic resonance spectroscopy.* Ph.D. thesis, Stellenbosch University, 2013.

[13] Raue, A., Kreutz, C., Maiwald, T., Bachmann, J., Schilling, M., Klingmüller, U. and Timmer, J.: Structural and practical identifiability analysis of partially observed dynamical models by exploiting the profile likelihood. *Bioinformatics*, vol. 25, no. 15, pp. 1923–1929, 2009. ISSN 13674803.

[14] Snoep, J.L. and Westerhoff, H.V.: From isolation to integration, a systems biology approach for building the Silicon Cell. *Systems Biology*, vol. 13, no. January, pp. 13–30, 2005.

[15] Rivas, G. and Minton, A.P.: Macromolecular Crowding In Vitro, In Vivo, and In Between. *Trends in Biochemical Sciences*, vol. 41, no. 11, pp. 970–981, 2016. ISSN 13624326.

[16] Kuznetsova, I., Zaslavsky, B., Breydo, L., Turoverov, K. and Uversky, V.: Beyond the Excluded Volume Effects: Mechanistic Complexity of the Crowded Milieu. *Molecules*, vol. 20, no. 1, pp. 1377–1409, 2015. ISSN 1420-3049.

[17] Feig, M., Harada, R., Mori, T., Yu, I., Takahashi, K. and Sugita, Y.: Complete atomistic model of a bacterial cytoplasm for integrating physics, biochemistry, and systems biology. *Journal of Molecular Graphics and Modelling*, vol. 58, pp. 1–9, 2015. ISSN 18734243.

[18] Balcells, C., Pastor, I., Pitulice, L. and Via-nadal, M.: Macromolecular crowding upon in vivo like enzyme kinetics: effect of enzyme-obstacle siz. *New Front. Chem.*, vol. 24, no. 1, pp. 3–16, 2015.

[19] Aumiller, W.M., Davis, B.W., Hatzakis, E. and Keating, C.D.: Interactions of macromolecular crowding agents and cosolutes with small-molecule substrates: Effect on horseradish peroxidase activity with two different substrates. *Journal of Physical Chemistry B*, vol. 118, no. 36, pp. 10624–10632, 2014. ISSN 15205207.

[20] Pastor, I., Pitulice, L., Balcells, C., Vilaseca, E., Madurga, S., Isvoran, A., Cascante, M. and Mas, F.: Effect of crowding by Dextrans in enzymatic reactions. *Biophysical Chemistry*, vol. 185, pp. 8–13, 2014. ISSN 03014622.

[21] Minton, A.P.: Molecular Crowding: Analysis of Effects of High Concentrations of Inert Cosolutes on Biochemical Equilibria and Rates in Terms of Volume Exclusion. *Methods in Enzymology*, vol. 295, pp. 127–149, 1998.

[22] Ralston, G.B.: Effects of "crowding" in protein solutions. *Journal of Chemical Education*, vol. 67, no. 10, pp. 857–860, 1990. ISSN 00219584.

[23] Hata, Y., Sawada, T. and Serizawa, T.: Macromolecular crowding for materials-directed controlled self-assembly. *Journal of Materials Chemistry B*, vol. 6, no. 40, pp. 6344–6359, 2018. ISSN 2050750X.

[24] Van Den Berg, J., Boersma, A.J. and Poolman, B.: Microorganisms maintain crowding homeostasis. *Nature Reviews Microbiology*, vol. 15, no. 5, pp. 309–318, 2017. ISSN 17401534.

[25] Zimmerman, S.B. and Minton, A.P.: Macromolecular Crowding: Biochemical, Biophysical, and Physiological Consequences. *Annual Review of Biophysics and Biomolecular Structure*, vol. 22, no. 1, pp. 27–65, 1993.

[26] Minton, A.P.: The Influence of Macromolecular Crowding and Macromolecular Confinement on Biochemical Reactions in Physiological Media. *Journal of Biological Chemistry*, vol. 276, no. 14, pp. 10577–10580, 2001. ISSN 00219258.

[27] Sasahara, K., McPhie, P. and Minton, A.P.: Effect of dextran on protein stability and conformation attributed to macromolecular crowding. *Journal of Molecular Biology*, vol. 326, no. 4, pp. 1227–1237, 2003. ISSN 00222836.

[28] Shahid, S., Ahmad, F., Hassan, M.I. and Islam, A.: Mixture of Macromolecular Crowding Agents Has a Non-additive Effect on the Stability of Proteins. *Applied Biochemistry and Biotechnology*, vol. 188, no. 4, pp. 927–941, 2019. ISSN 15590291.

[29] Minton, A.P.: Quantitative assessment of the relative contributions of steric repulsion and chemical interactions to macromolecular crowding. *Biopolymers*, vol. 99, no. 4, pp. 239–244, 2013. ISSN 00063525.

[30] Silverstein, T.P. and Slade, K.: Effects of Macromolecular Crowding on Biochemical Systems. *Journal of Chemical Education*, vol. 96, no. 11, pp. 2476–2487, 2019. ISSN 0021-9584.

[31] Miklos, A.C., Sarkar, M., Wang, Y. and Pielak, G.J.: Protein crowding tunes protein stability. *Journal of the American Chemical Society*, vol. 133, no. 18, pp. 7116–7120, 2011. ISSN 00027863.

[32] Winther, K., Tree, J.J., Tollervey, D. and Gerdes, K.: VapCs of Mycobacterium tuberculosis cleave RNAs essential for translation. *Nucleic Acids Research*, vol. 44, no. 20, pp. 9860–9871, 2016. ISSN 13624962.

[33] Zhou, H.-X., Rivas, G. and Minton, A.P.: Macromolecular Crowding and Confinement: Biochemical, Biophysical, and Potential Physiological Consequences. *Annual Review of Biophysics*, vol. 37, no. 1, pp. 375–397, 2008. ISSN 1936-122X.

[34] Gnutt, D. and Ebbinghaus, S.: The macromolecular crowding effect - From in vitro into the cell. *Biological Chemistry*, vol. 397, no. 1, pp. 37–44, 2016. ISSN 14374315.

[35] Miklos, A.C., Li, C., Sharaf, N.G. and Pielak, G.J.: Volume exclusion and soft interaction effects on protein stability under crowded conditions. *Biochemistry*, vol. 49, no. 33, pp. 6984–6991, 2010. ISSN 00062960.

[36] Minton, A.P.: Explicit Incorporation of Hard and Soft Protein-Protein Interactions into Models for Crowding Effects in Protein Mixtures. 2. Effects of Varying Hard and Soft Interactions upon Prototypical Chemical Equilibria. *Journal of Physical Chemistry B*, vol. 121, no. 22, pp. 5515–5522, 2017. ISSN 15205207.

[37] Schlesinger, A.P., Wang, Y., Tadeo, X., Millet, O. and Pielak, G.J.: Macromolecular crowding fails to fold a globular protein in cells. *Journal of the American Chemical Society*, vol. 133, no. 21, pp. 8082–8085, 2011. ISSN 00027863.

[38] Dix, J.A. and Verkman, A.: Crowding Effects on Diffusion in Solutions and Cells. *Annual Review of Biophysics*, vol. 37, no. 1, pp. 247–263, 2008. ISSN 1936-122X.

[39] Banks, D.S. and Fradin, C.: Anomalous diffusion of proteins due to molecular crowding. *Biophysical Journal*, vol. 89, no. 5, pp. 2960–2971, 2005. ISSN 00063495.

[40] Weiss, M.: Crowding, diffusion, and biochemical reactions. *International Review of Cell and Molecular Biology*, vol. 307, pp. 383–417, 2014. ISSN 19376448.

[41] Hou, S., Ziebacz, N., Kalwarczyk, T., Kaminski, T.S., Wieczorek, S.A. and Holyst, R.: Influence of nano-viscosity and depletion interactions on cleavage of DNA by enzymes in glycerol and poly(ethylene glycol) solutions: Qualitative analysis. *Soft Matter*, vol. 7, no. 7, pp. 3092–3099, 2011. ISSN 1744683X.

[42] Weiss, M., Elsner, M., Kartberg, F. and Nilsson, T.: Anomalous subdiffusion is a measure for cytoplasmic crowding in living cells. *Biophysical Journal*, vol. 87, no. 5, pp. 3518–3524, 2004. ISSN 00063495.

[43] Schneider, S.H., Lockwood, S.P., Hargreaves, D.I., Slade, D.J., Loconte, M.A., Logan, B.E., McLaughlin, E.E., Conroy, M.J. and Slade, K.M.: Slowed Diffusion and Excluded Volume Both Contribute to the Effects of Macromolecular Crowding on Alcohol Dehydrogenase Steady-State Kinetics. *Biochemistry*, vol. 54, no. 38, pp. 5898–5906, 2015. ISSN 15204995.

[44] Spitzer, J.: Emergence of Life on Earth: A Physicochemical Jigsaw Puzzle. *Journal of Molecular Evolution*, vol. 84, no. 1, pp. 1–7, 2017. ISSN 00222844.

[45] Marenduzzo, D., Finan, K. and Cook, P.R.: The depletion attraction: An underappreciated force driving cellular organization. *Journal of Cell Biology*, vol. 175, no. 5, pp. 681–686, 2006. ISSN 00219525.

[46] Parker, J.C. and Craig Colclasure, G.: Macromolecular crowding and volume perception in dog red cells. *Molecular and Cellular Biochemistry*, vol. 114, no. 1-2, pp. 9–11, 1992. ISSN 03008177.

[47] Joyner, R.P., Tang, J.H., Helenius, J., Dultz, E., Brune, C., Holt, L.J., Huet, S., Müller, D.J. and Weis, K.: A glucose-starvation response regulates the diffusion of macromolecules. *eLife*, vol. 5, p. e09376, 2016. ISSN 2050084X.

[48] Boersma, A.J., Zuhorn, I.S. and Poolman, B.: A sensor for quantification of macromolecular crowding in living cells. *Nature Methods*, vol. 12, no. 3, pp. 227–229, 2015. ISSN 15487105.

[49] Gnutt, D., Gao, M., Brylski, O., Heyden, M. and Ebbinghaus, S.: Excluded-Volume Effects in Living Cells. *Angewandte Chemie International Edition*, vol. 54, no. 8, pp. 2548–2551, 2015. ISSN 14337851.

[50] Bounedjah, O., Hamon, L., Savarin, P., Desforges, B., Curmi, P.A. and Pastré, D.: Macromolecular crowding regulates assembly of mRNA stress granules after osmotic stress: New role for compatible osmolytes. *Journal of Biological Chemistry*, vol. 287, no. 4, pp. 2446–2458, 2012. ISSN 00219258.

[51] Wirth, A.J., Platkov, M. and Gruebele, M.: Temporal variation of a protein folding energy landscape in the cell. *Journal of the American Chemical Society*, vol. 135, no. 51, pp. 19215–19221, 2013. ISSN 00027863.

[52] Dhar, A., Samiotakis, A., Ebbinghaus, S., Nienhaus, L., Homouz, D., Gruebele, M. and Cheung, M.S.: Structure, function, and folding of phosphoglycerate kinase are strongly perturbed by macromolecular crowding. *Proceedings of the National Academy of Sciences of the United States of America*, vol. 107, no. 41, pp. 17586–17591, 2010. ISSN 0027-8424.

[53] Petrovska, I., Nüske, E., Munder, M.C., Kulasegaran, G., Malinovska, L., Kroschwald, S., Richter, D., Fahmy, K., Gibson, K., Verbavatz, J.M. and Alberti, S.: Filament formation by metabolic enzymes is a specific adaptation to an advanced state of cellular starvation. *eLife*, vol. 3, p. e02409, 2014. ISSN 2050084X.

[54] Jiang, M. and Guo, Z.: Effects of macromolecular crowding on the intrinsic catalytic efficiency and structure of enterobactin-specific isochorismate synthase. *Journal of the American Chemical Society*, vol. 129, no. 4, pp. 730–731, 2007. ISSN 00027863.

[55] Balcells, C., Pastor, I., Vilaseca, E., Madurga, S., Cascante, M. and Mas, F.: Macromolecular crowding effect upon in vitro enzyme kinetics: Mixed activation-diffusion control of the oxidation of NADH by pyruvate catalyzed by lactate dehydrogenase. *Journal of Physical Chemistry B*, vol. 118, no. 15, pp. 4062–4068, 2014. ISSN 15205207.

[56] Poggi, C. and Slade, K.: Macromolecular Crowding and the Steady-State Kinetics of Malate Dehydrogenase. *Biochemistry*, vol. 54, no. 2, pp. 260–267, 2015.

[57] Pozdnyakova, I. and Wittung-Stafshede, P.: Non-linear effects of macromolecular crowding on enzymatic activity of multi-copper oxidase. *Biochimica et Biophysica Acta - Proteins and Proteomics*, vol. 1804, no. 4, pp. 740–744, 2010. ISSN 15709639.

[58] Morán-Zorzano, M.T., Viale, A.M., Muñoz, F.J., Alonso-Casajús, N., Eydallín, G.G., Zugasti, B., Baroja-Fernández, E. and Pozueta-Romero, J.: Escherichia coli AspP activity is enhanced by macromolecular crowding and by both glucose-1,6-bisphosphate and nucleotide-sugars. *FEBS Letters*, vol. 581, no. 5, pp. 1035–1040, 2007. ISSN 00145793.

[59] Wilcox, A.E., LoConte, M.A. and Slade, K.M.: Effects of macromolecular crowding on alcohol dehydrogenase activity are substrate-dependent. *Biochemistry*, vol. 55, no. 25, pp. 3550–3558, 2016. ISSN 15204995.

[60] Shahid, S., Hassan, M.I., Islam, A. and Ahmad, F.: Size-dependent studies of macromolecular crowding on the thermodynamic stability, structure and functional activity of proteins: in vitro and in silico approaches. *Biochimica et Biophysica Acta (BBA) - General Subjects*, vol. 1861, no. 2, pp. 178–197, 2016. ISSN 03044165.

[61] Barabási, A.L. and Oltvai, Z.N.: Network biology: Understanding the cell's functional organization. *Nature Reviews Genetics*, vol. 5, no. 2, pp. 101–113, 2004. ISSN 14710056.

[62] Bruggeman, F.J. and Westerhoff, H.V.: The nature of systems biology. *Trends in Microbiology*, vol. 15, no. 1, pp. 45–50, 2007. ISSN 0966842X.

[63] Westerhoff, H.V. and Alberghina, L.: Systems Biology: Did we know it all along? *Topics in Current Genetics*, vol. 13, pp. 3–9, 2005. ISSN 1610-2096.

[64] Shahzad, K. and J. Loor, J.: Application of Top-Down and Bottom-up Systems Approaches in Ruminant Physiology and Metabolism. *Current Genomics*, vol. 13, no. 5, pp. 379–394, 2012. ISSN 13892029.

[65] Rohwer, J.M.: Kinetic modelling of plant metabolic pathways. *Journal of Experimental Botany*, vol. 63, no. 6, pp. 2275–2292, 2012. ISSN 00220957.

[66] Jeske, L., Placzek, S., Schomburg, I., Chang, A. and Schomburg, D.: BRENDA in 2019: A European ELIXIR core data resource. *Nucleic Acids Research*, vol. 47, no. D1, pp. D542–D549, 2019. ISSN 13624962.

[67] Wittig, U., Kania, R., Golebiewski, M., Rey, M., Shi, L., Jong, L., Algaa, E., Weidemann, A., Sauer-Danzwith, H., Mir, S., Krebs, O., Bittkowski, M., Wetsch, E., Rojas, I. and Müller, W.: SABIO-RK - Database for biochemical reaction kinetics. *Nucleic Acids Research*, vol. 40, no. D1, pp. 790–796, 2012. ISSN 03051048.

[68] Jaqaman, K. and Danuser, G.: Linking data to models: Data regression. *Nature Reviews Molecular Cell Biology*, vol. 7, no. 11, pp. 813–819, 2006. ISSN 14710072.

[69] Raue, A., Karlsson, J., Saccomani, M.P., Jirstrand, M. and Timmer, J.: Comparison of approaches for parameter identifiability analysis of biological systems. *Bioinformatics*, vol. 30, no. 10, pp. 1440–1448, 2014. ISSN 14602059.

[70] Swanepoel, C.J.: *A systematic investigation into the quantitative effect of pH changes on the upper glycolytic enzymes of Escherichia coli and Saccharomyces cerevisiae*. Master's thesis, Stellenbosch University, 2018.

[71] Ashyraliyev, M., Fomekong-Nanfack, Y., Kaandorp, J.A. and Blom, J.G.: Systems biology: Parameter estimation for biochemical models. *FEBS Journal*, vol. 276, no. 4, pp. 886–902, 2009. ISSN 1742464X.

[72] Kreutz, C. and Timmer, J.: Systems biology: Experimental design. *FEBS Journal*, vol. 276, no. 4, pp. 923–942, 2009. ISSN 1742464X.

[73] Little, M.P., Heidenreich, W.F. and Li, G.: Parameter identifiability and redundancy: Theoretical considerations. *PLoS ONE*, vol. 5, no. 1, p. e8915, 2010. ISSN 19326203.

[74] Berthoumieux, S., Brilli, M., Kahn, D., de Jong, H. and Cinquemani, E.: On the identifiability of metabolic network models. *Journal of Mathematical Biology*, vol. 67, no. 6-7, pp. 1795–1832, 2013. ISSN 03036812.

[75] Bellu, G., Saccomani, M.P., Audoly, S. and D'Angiò, L.: DAISY: A new software tool to test global identifiability of biological and physiological systems. *Computer Methods and Programs in Biomedicine*, vol. 88, no. 1, pp. 52–61, 2007. ISSN 01692607.

[76] Pohjanpalo, H.: System identifiability based on the power series expansion of the solution. *Mathematical Biosciences*, vol. 41, no. 1-2, pp. 21–33, 1978. ISSN 00255564.

[77] Raue, A., Becker, V., Klingmüller, U. and Timmer, J.: Identifiability and observability analysis for experimental design in nonlinear dynamical models. *Chaos*, vol. 20, no. 4, pp. 1–8, 2010. ISSN 10541500.

[78] Hines, K.E., Middendorf, T.R. and Aldrich, R.W.: Determination of parameter identifiability in nonlinear biophysical models: A bayesian approach. *Journal of General Physiology*, vol. 143, no. 3, pp. 401–416, 2014. ISSN 00221295.

[79] Bradford, M.M.: A rapid and sensitive method for the quantitation of microgram quantities of protein utilizing the principle of protein-dye binding. *Analytical biochemistry*, vol. 72, pp. 248–254, 1976. ISSN 00032697.

[80] Badenhorst, M., Barry, C.J., Swanepoel, C.J., van Staden, C.T., Wissing, J. and Rohwer, J.M.: Workflow for Data Analysis in Experimental and Computational Systems Biology: Using Python as 'Glue'. *Processes*, vol. 7, no. 7, p. 460, 2019. ISSN 2227-9717.

[81] Rohwer, J.M., Hanekom, A.J. and Hofmeyr, J.-h.S.: A Universal Rate Equation for Systems Biology. In: *Proceed 2nd Intern ESCEC Symp*, pp. 175–188. Beilstein Institut zur Foerderung der Chemischen Wissenschaften, 2007. ISSN 1471-0072.

[82] Banuelos, M., Gancedo, C. and Gancedo, J.M.: Activation by phosphate of yeast phosphofructokinase. *Journal of Biological Chemistry*, vol. 252, no. 18, pp. 6394–6398, 1977. ISSN 00219258.

[83] Eicher, J.J., Snoep, J.L. and Rohwer, J.M.: Determining Enzyme Kinetics for Systems Biology with Nuclear Magnetic Resonance Spectroscopy. *Metabolites*, vol. 2, pp. 818–843, 2012. ISSN 2218-1989.

[84] Teusink, B., Passarge, J., Reijenga, C.A., Esgalhado, E., Van Der Weijden, C.C., Schepper, M., Walsh, M.C., Bakker, B.M., Van Dam, K., Westerhoff, H.V. and Snoep, J.L.: Can yeast glycolysis be understood terms of vitro kinetics of the constituent enzymes? Testing biochemistry. *European Journal of Biochemistry*, vol. 267, no. 17, pp. 5313–5329, 2000. ISSN 00142956.

[85] Olivier, B.G., Rohwer, J.M. and Hofmeyr, J.H.S.: Modelling cellular systems with PySCeS. *Bioinformatics*, vol. 21, no. 4, pp. 560–561, 2005. ISSN 13674803.

[86] Newville, M., Ingargiola, A., Stensitzki, T. and Allen, D.B.: LMFIT: Non-Linear Least-Square Minimization and Curve-Fitting for Python. *Zenodo*, 2014.

[87] Du Prel, J.B., Hommel, G., Röhrig, B. and Blettner, M.: Confidence interval or p-value?: part 4 of a series on evaluation of scientific publications. *Dtsch. Arztebl. Int.*, vol. 106, no. 19, pp. 335–339, 2009. ISSN 00121207.

[88] Nakagawa, S. and Cuthill, I.C.: Effect size, confidence interval and statistical significance: A practical guide for biologists. *Biological Reviews*, vol. 82, no. 4, pp. 591–605, 2007. ISSN 14647931.

[89] Van Den Brink, J., Canelas, A.B., Van Gulik, W.M., Pronk, J.T., Heijnen, J.J., De Winde, J.H. and Daran-Lapujade, P.: Dynamics of glycolytic regulation during adaptation of Saccharomyces cerevisiae to fermentative metabolism. *Applied and Environmental Microbiology*, vol. 74, no. 18, pp. 5710–5723, 2008. ISSN 00992240.

[90] Reuter, R., Naumann, M., Bär, J., Haferburg, D. and Kopperschläger, G.: Purification, molecular and kinetic characterization of phosphofructokinase-I from the yeast Schizosaccharomyces pombe: Evidence for an unusual subunit composition. *Yeast*, vol. 16, no. 14, pp. 1273–1285, 2000. ISSN 0749503X.

[91] Green, J.B., Wright, A.P., Cheung, W.Y., Lancashire, W.E. and Hartley, B.S.: The structure and regulation of phosphoglucose isomerase in Saccharomyces cerevisiae. *MGG Molecular & General Genetics*, vol. 215, no. 1, pp. 100–106, 1988. ISSN 00268925.

[92] Rose, I.A.: Mechanism of the Aldose-Ketose Isomerase Reactions. *Advances in Enzymology and Related Areas of Molecular Biology*, vol. 43, pp. 491–517, 2006. ISSN 0065-258X.

[93] Bruch, P., Schnackerz, K.D. and Gracy, R.W.: Matrix-Bound Phosphoglucose Isomerase: Formation and Properties of Monomers and Hybrids. *European Journal of Biochemistry*, vol. 68, no. 1, pp. 153–158, 1976. ISSN 14321033.

[94] Sols, A., Castano, J.G., Aragon, J.J., Domenech, C., Lazo, P.A. and Nieto, A.: Multimodulation of Phosphofructokinases. In: H. Holzer (ed.), *Metabolic Interconversions of Enzymes 1980*, pp. 111–123. 1981.

[95] Kopperschläger, G., Bär, J., Nissler, K. and Hofmann, E.: Physicochemical Parameters and Subunit Composition of Yeast Phosphofructokinase. *European Journal of Biochemistry*, vol. 81, no. 2, pp. 317–325, 1977. ISSN 14321033.

[96] Bárcena, M., Radermacher, M., Bär, J., Kopperschläger, G. and Ruiz, T.: The structure of the ATP-bound state of S. cerevisiae phosphofructokinase determined by cryo-electron microscopy. *Journal of Structural Biology*, vol. 159, no. 1, pp. 135–143, 2007. ISSN 10478477.

[97] Laurent, P., Seydoux, M. and Dessen, F.: Allosteric regulation of yeast phosphofructokinase. Correlation between equilibrium binding, spectroscopic and kinetic data. *Journal of Biological Chemistry*, vol. 254, no. 16, pp. 7515–7520, 1979.

[98] Thoke, H.S., Bagatolli, L.A. and Olsen, L.F.: Effect of macromolecular crowding on the kinetics of glycolytic enzymes and the behaviour of glycolysis in yeast. *Integrative Biology (United Kingdom)*, vol. 10, no. 10, pp. 587–597, 2018. ISSN 17579708.

[99] Sharp, K.A.: Analysis of the size dependence of macromolecular crowding shows that smaller is better. *Proceedings of the National Academy of Sciences*, vol. 112, no. 26, pp. 7990–7995, 2015. ISSN 0027-8424.

[100] Zhou, B.R., Liang, Y., Du, F., Zhou, Z. and Chen, J.: Mixed macromolecular crowding accelerates the oxidative refolding of reduced, denatured lysozyme: Implications for protein folding in intracellular environments. *Journal of Biological Chemistry*, vol. 279, no. 53, pp. 55109–55116, 2004. ISSN 00219258.

[101] Biswas, S., Kundu, J., Mukherjee, S.K. and Chowdhury, P.K.: Mixed Macromolecular Crowding: A Protein and Solvent Perspective. *ACS Omega*, vol. 3, no. 4, pp. 4316–4330, 2018. ISSN 24701343.